



Superconducting Ion Source Development in Berkeley

Daniela Leitner, S. Caspi, P. Ferracin, C.M. Lyneis,
S. Prestemon, G.L. Sabbi, D.S. Todd, F. Trillaud

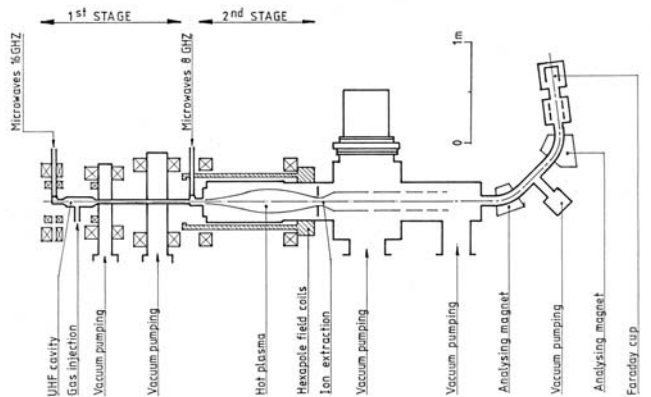
- Motivation for developing superconducting ECR ion sources
- Key parameters for the performance of an ECR
- VENUS Source Project
- Some results and status of the VENUS ECR ion source
- Future ECR ion source – Path to 56 GHz ECRIS

HIAT 2009, Venice, Italy



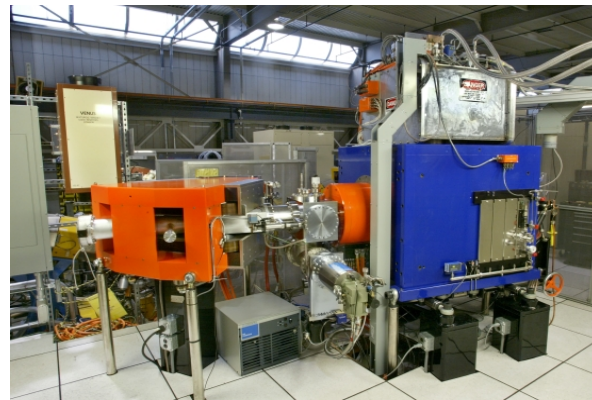
ECR ion sources have made remarkable improvements over the last few decades, but the demand for increased intensities of highly charged heavy ions continues to grow

Supermafios (Geller, 1974) 15 μA of O^{6+}



Factor
200
increase
→

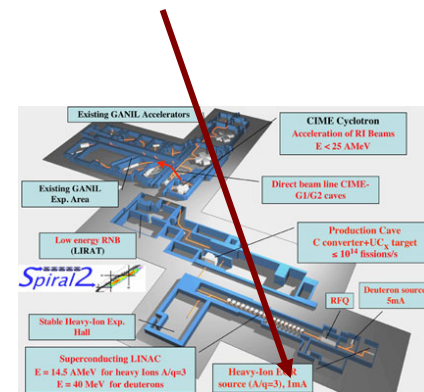
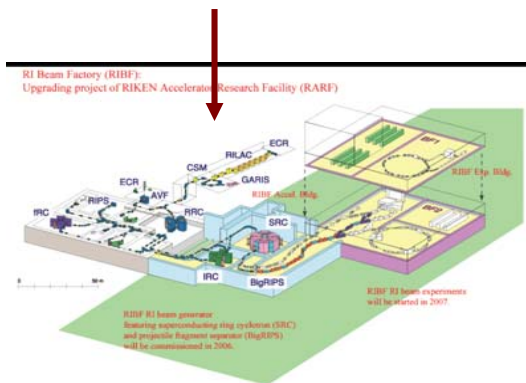
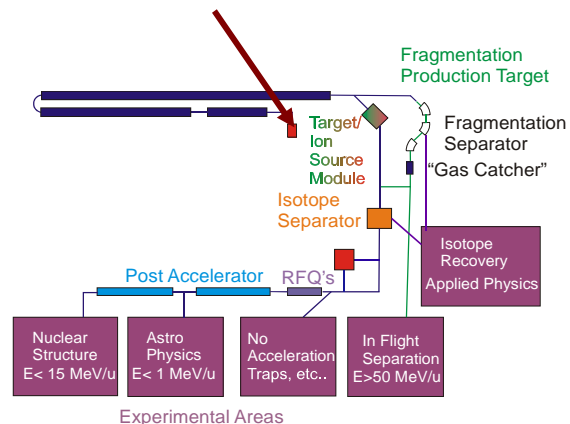
VENUS (2007) 2850 μA of O^{6+}



VENUS, FRIB MSU, USA

SC-ECRIS, RIKEN, Japan

SPIRAL 2, GANIL, France



270 μA U^{33+} and 270 μA U^{34+}

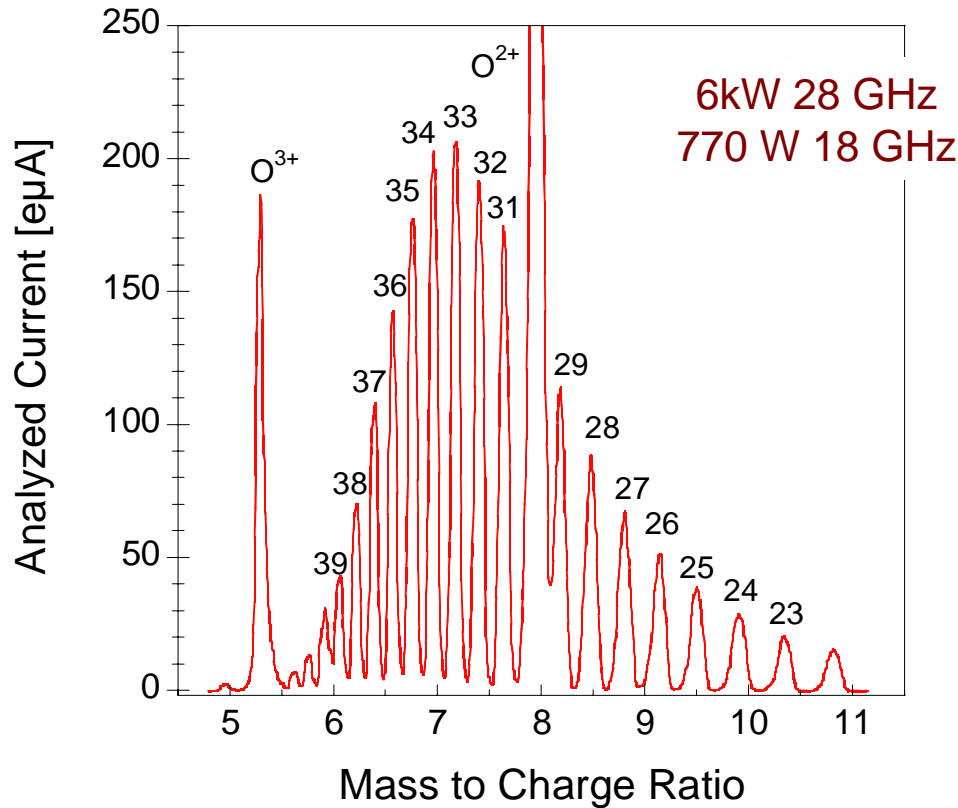
525 μA U^{35+}

1mA Ar^{12+}



The demonstrated VENUS source performance shows that these ion beam intensity requirements are possible

High Intensity Uranium Production



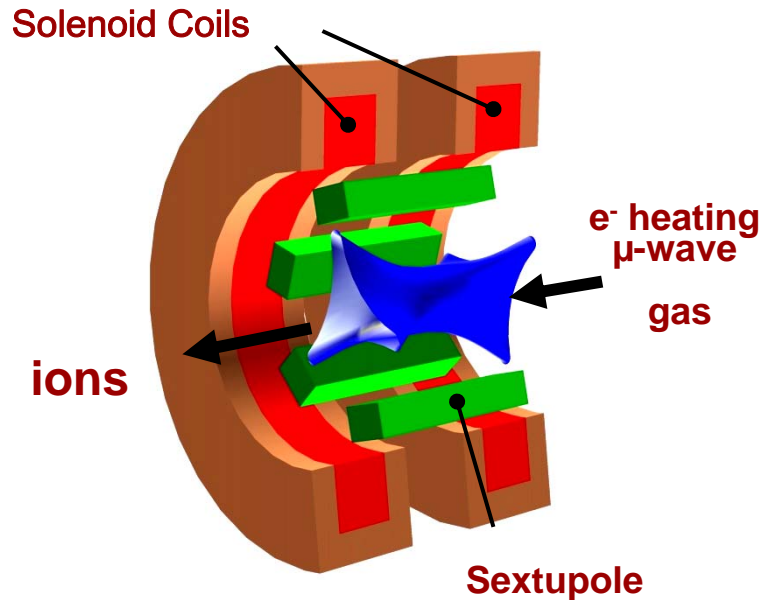
	VENUS 28GHz or 28+18 GHz
O ⁶⁺	2860 e μ A
O ⁷⁺	850 e μ A
O ⁸⁺	~ 400 e μ A
Ar ¹²⁺	860 e μ A
Ar ¹⁷⁺	36 e μ A
Xe ³⁵⁺	28 e μ A
Xe ⁴²⁺	.5 e μ A
U ³⁴⁺	200 e μ A
U ⁴⁷⁺	5 e μ A



Required temperature of 2100 C in a 4 T B field

Higher magnetic fields and higher frequencies are the key to higher performance

Minimum-B field Confinement



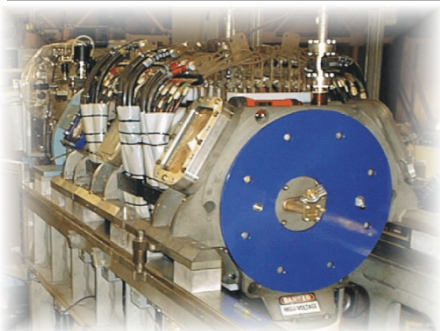
$$n_e \propto \omega_{rf}^2$$

$$q_{opt} \propto \log \omega^3$$

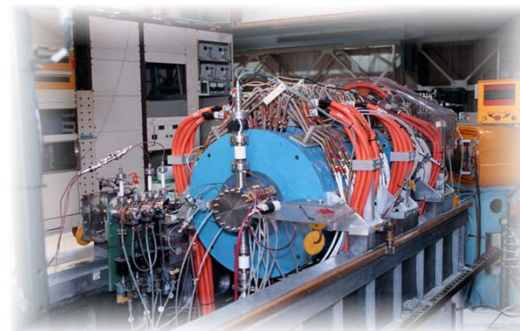
Resonant electron heating

$$\omega_e = \frac{e \cdot B}{m} = \omega_{rf}$$

ECR (1983)
0.4 T, 0.6 kW, 6.4 GHz



AECR-U (1996)
1.7 T, 2.6 kW, 10 + 14 GHz

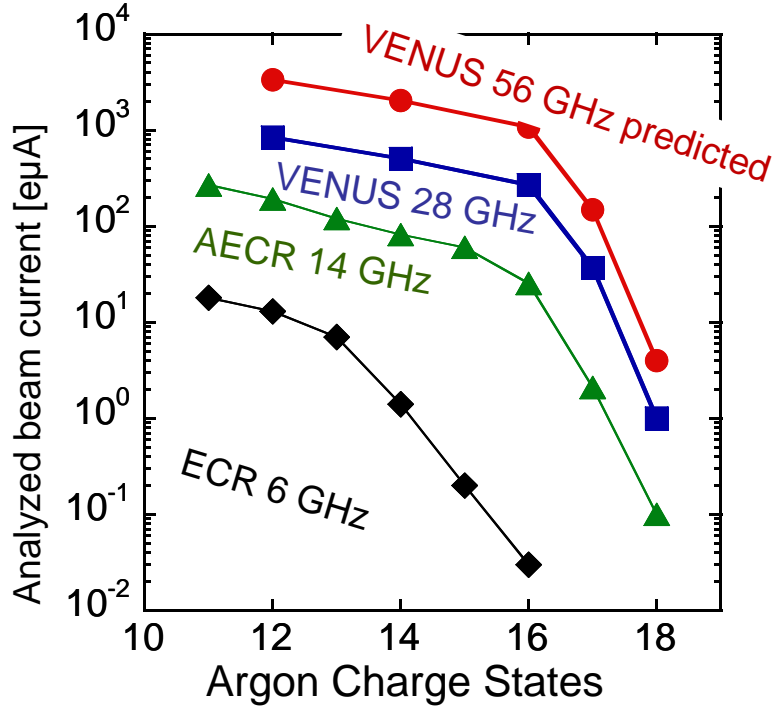


VENUS (2001)
4.0 T, 14 kW, 18 + 28 GHz





Higher magnetic fields and higher frequencies are the key to higher performance



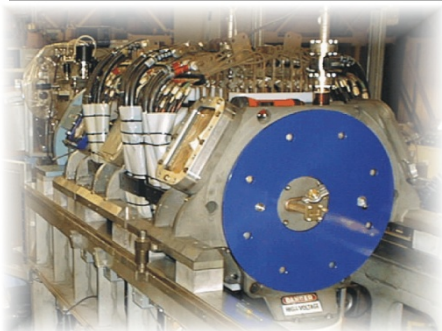
Normal conducting



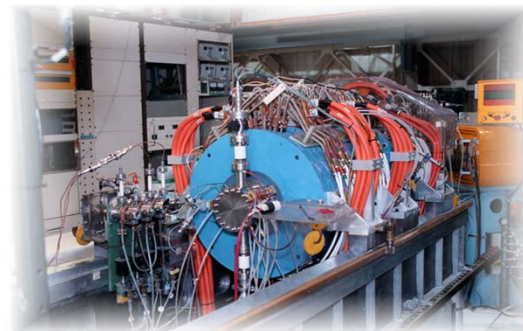
Super conducting

$$n_e \propto \$$$

ECR (1983)
0.4 T, 0.6 kW, 6.4 GHz



AECR-U (1996)
1.7 T, 2.6 kW, 10 + 14 GHz



VENUS (2001)
4.0 T, 14 kW, 18 + 28 GHz

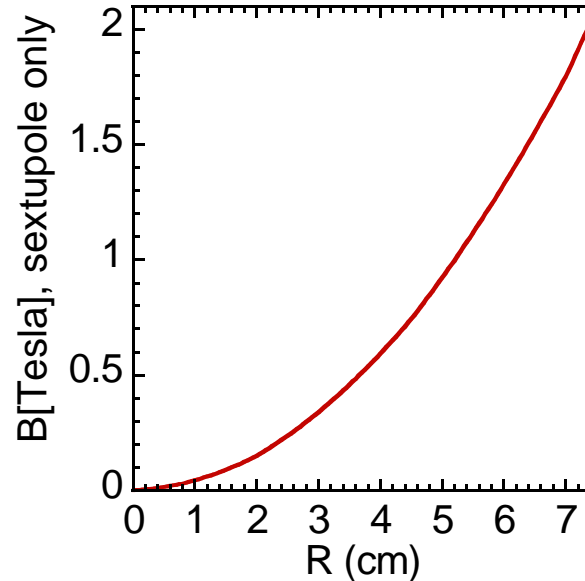
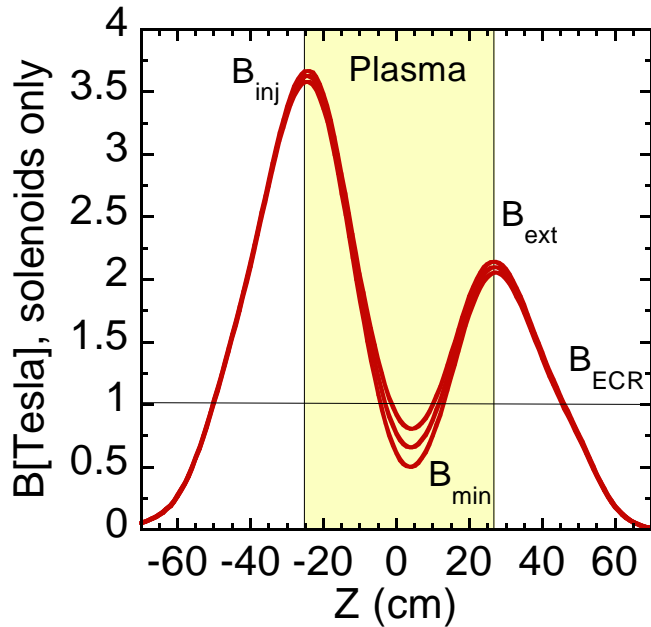


Challenges

- **Superconducting Magnet**
- **Cryogenic Technology**
- **X-rays from the Plasma**
- **Ion Beam Transport**



Superconducting Magnets: ECR Design 'Standard Model'



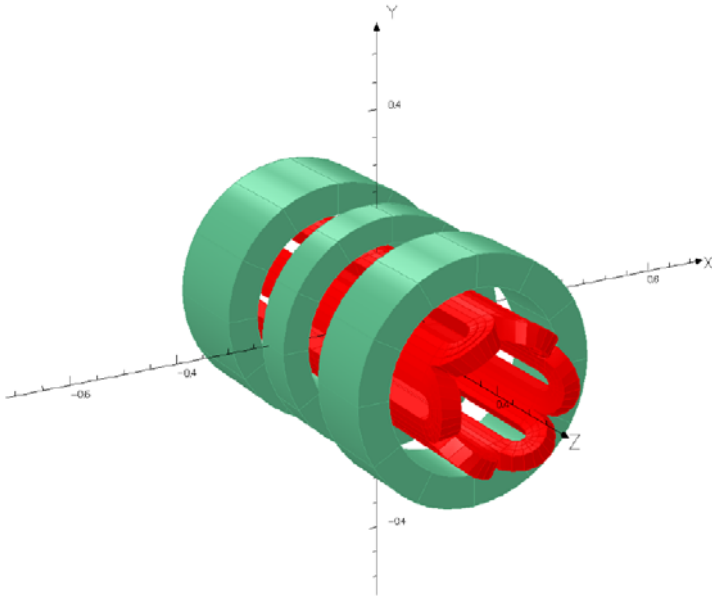
28 GHz 56 GHz

$B_{inj} \sim 4 \cdot B_{ecr}$	4T	8T
$B_{min} \sim 0.8 B_{ecr}$.5-.8 T	1-1.6 T
$B_{ext} \sim B_{rad}$	2T	4T
$B_{rad} \geq 2 B_{ecr}$	2T	4T
B_{ecr}	1T	2T

Magnetic Design		28 GHz	56 GHz
Max solenoid field	on the coil	6 T	12 T
	on axis	4 T	8 T
Max sextupole field	on the coil	7 T	15 T
	on plasma wall	2.1 T	4.2 T
Superconductor		NbTi	Nb ₃ Sn

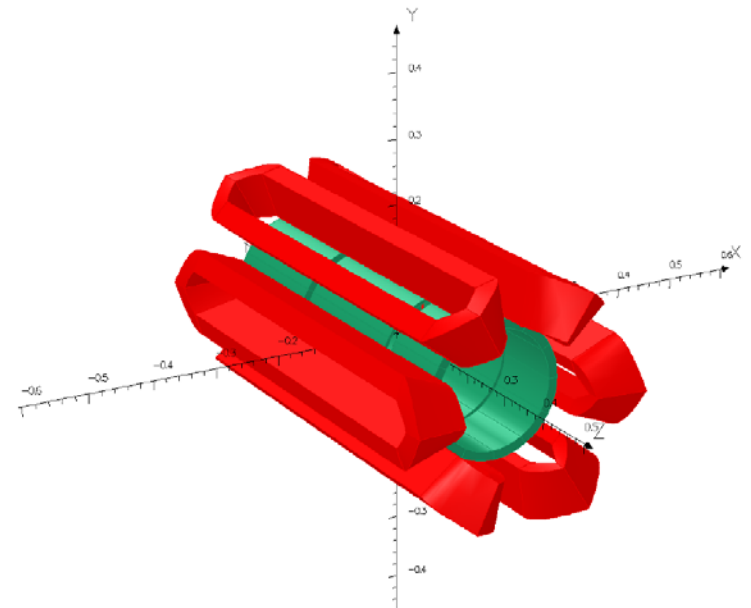
Superconducting Magnet Structure 56 GHz: two options

Sextupole-in-Solenoid Geometry (VENUS)



- Minimizes the peak fields in the sextupole coils
- Strong influence (forces) of the solenoid field on the sextupole ends

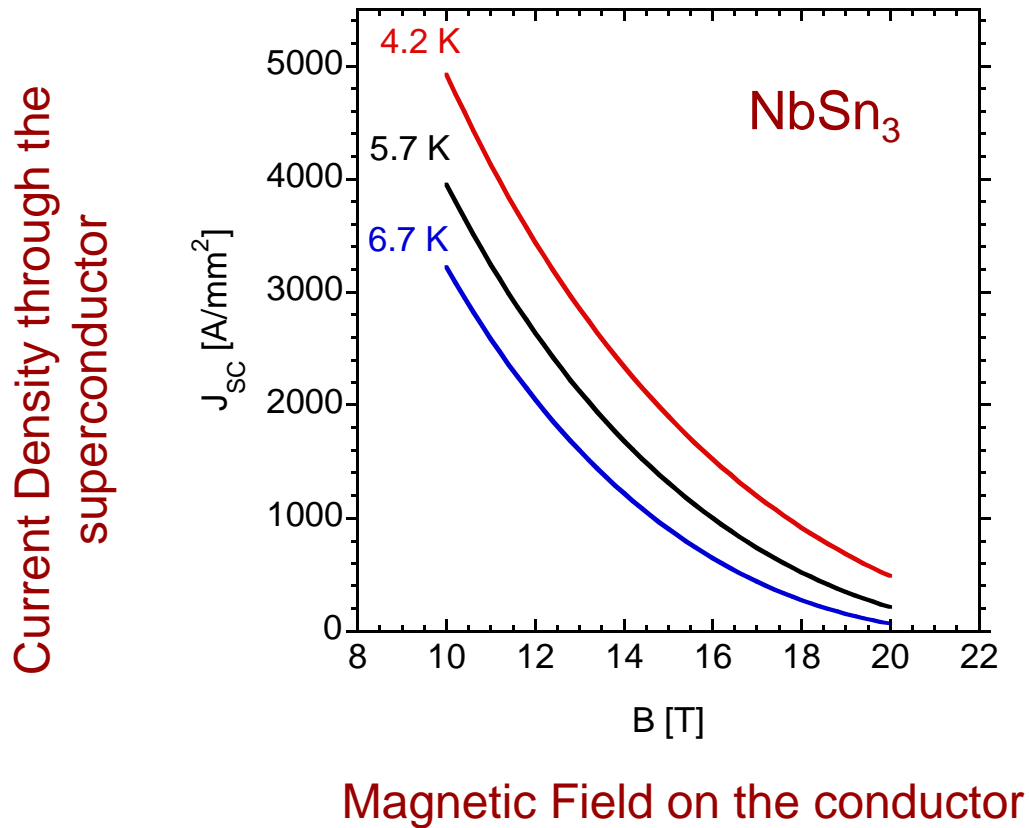
Solenoid-in-Sextupole Geometry (SECRAL)



- Minimizes the influence of the solenoid on the sextupole field
- Significantly higher field required for the sextupole magnet surface due to the larger radius of the coils
- Strong forces on the solenoid coils

Superconducting Magnet 56 GHz: Magnetic Analyses

Critical line and magnet load lines: NbSn₃

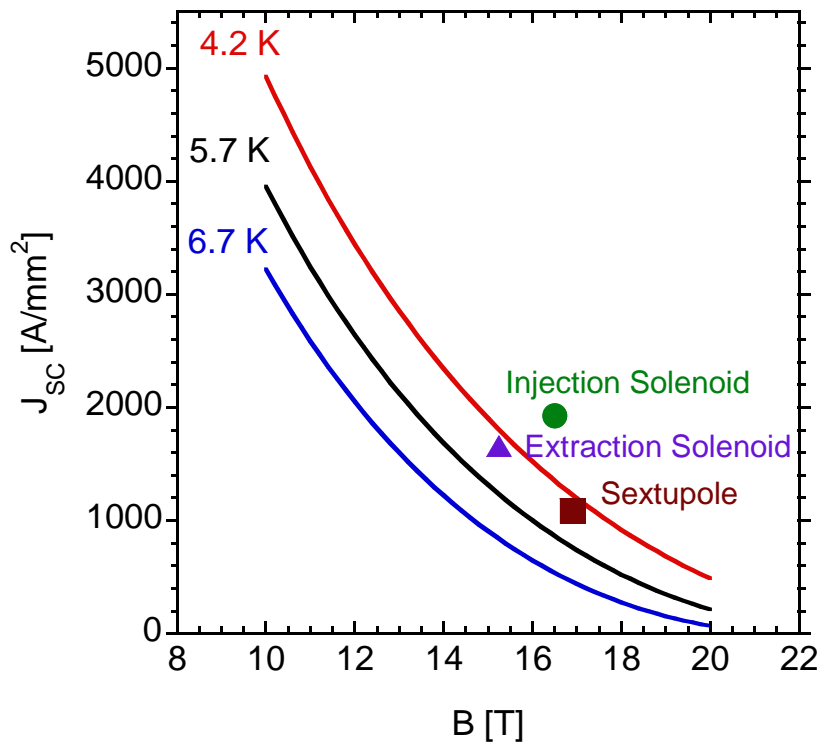


Superconducting Magnet Structure: Magnetic Analyses

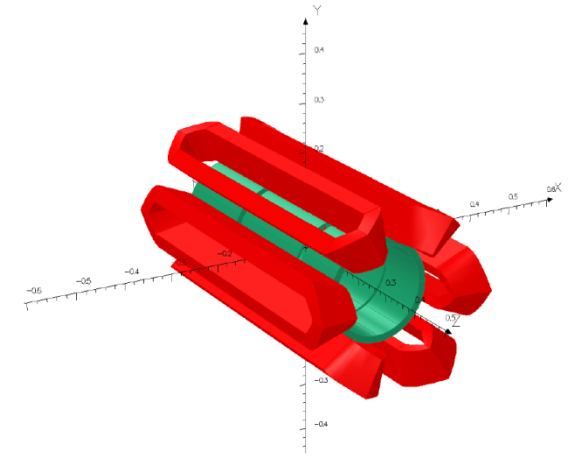
Goal: Achieve 4.2T on the plasma chamber wall radially
and 8 T and 4 T on axis

Solenoid-in-Sextupole

Current Density through the
superconductor



Magnetic Field on the conductor



•Magnetic field and current density requirements exceed the capability of NbSn₃

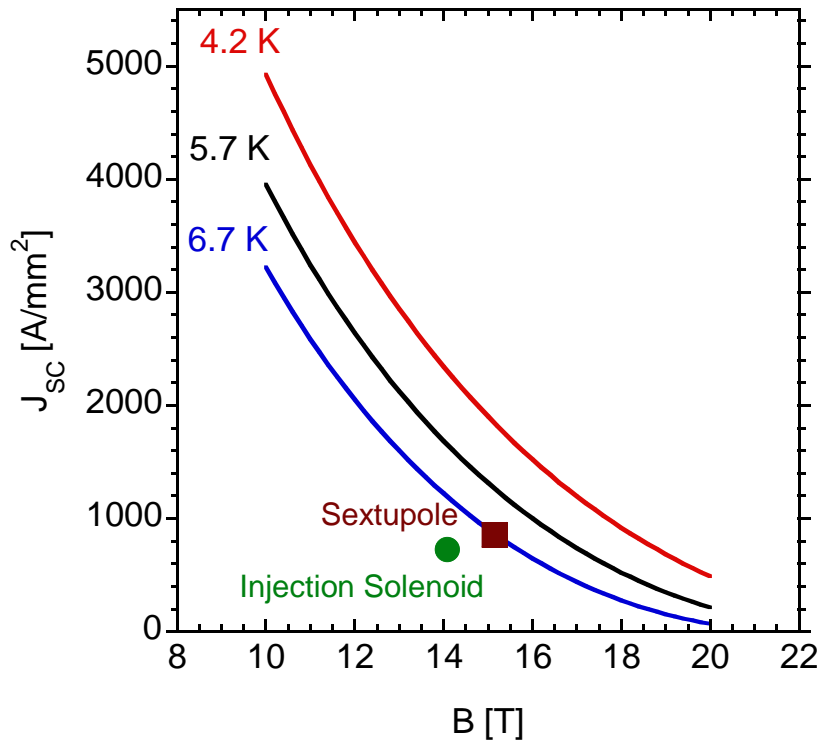
This geometry can be ruled out as candidate for a 56 GHz ECR ion source

Superconducting Magnet Structure: Magnetic Analyses

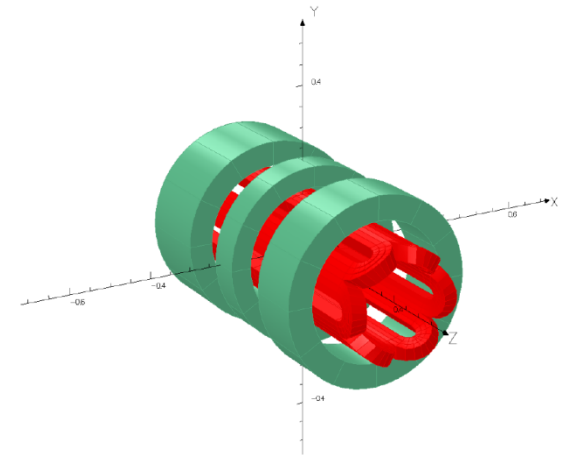
Goal: Achieve 4.2T on the plasma chamber wall radially
and 8 T and 4 T on axis

Sextupole-in-Solenoid

Current Density through the
superconductor



Magnetic Field on the conductor



- 2.5 Kelvin temperature margin for the Sextupole
- Operates at 86% of current limits

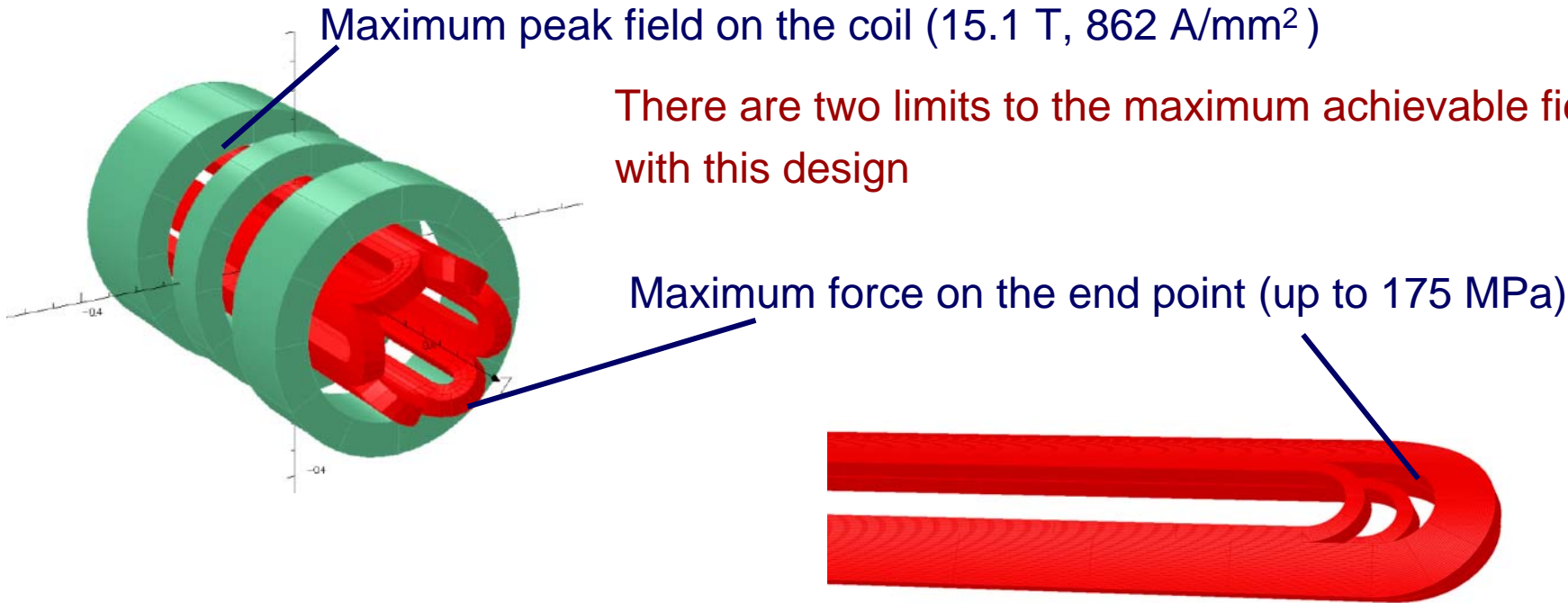
This geometry is challenging but feasible with current NbSn₃ technology

Sextupole-in-Solenoid: Clamping Structure

Maximum peak field on the coil (15.1 T , 862 A/mm^2)

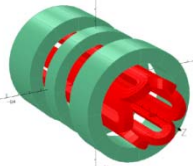
There are two limits to the maximum achievable field with this design

Maximum force on the end point (up to 175 MPa)

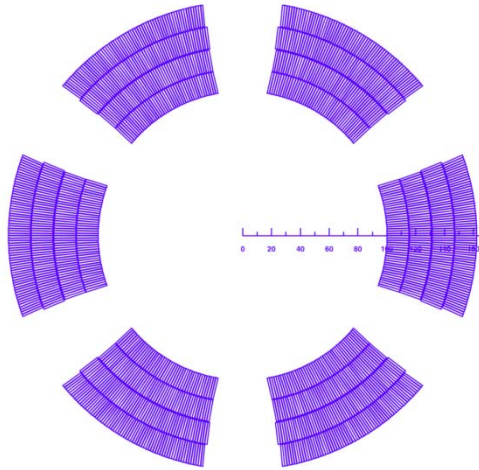


To control these forces

- In the end region each layer is subdivided in two blocks of conductors separated by end-spacers.
- The number of turns per block and the relative axial position of the end spacers were optimized to reduce the peak field in the end region.
- The coils are lengthen to reduce the peak field
- Shell type support structure



Sextupole-in-Solenoid: Sextupole Magnet



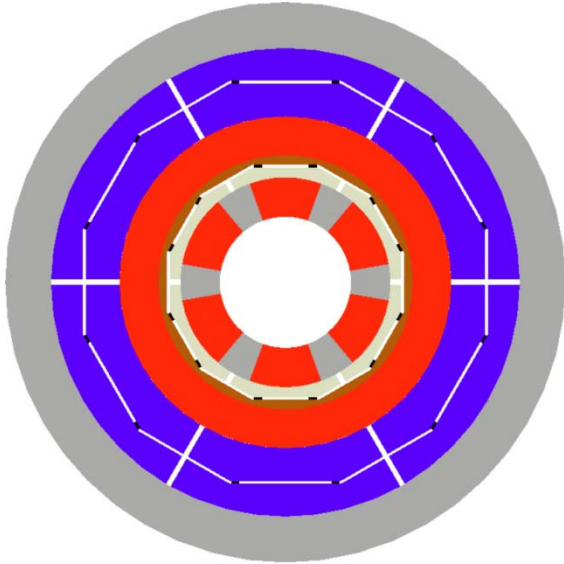
- 4-layer coils using cables (675 conductors/coil)
- The same cable design is currently used by the LARP program to develop high field quadrupoles for future LHC luminosity upgrades (peak fields 15 T)



Cable properties	
Strand Dia	0.8 mm
Fill factor	~ 33%
No strands	35
Cable	~ 15.2x1.5 mm

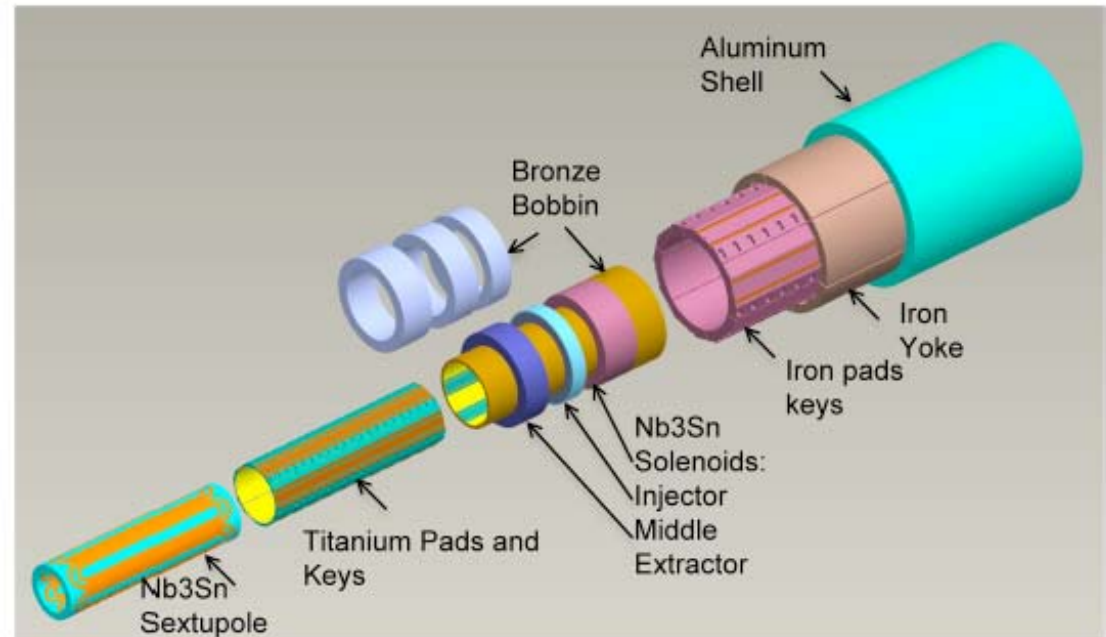
- The cable design requires high 8.2kA current leads, the 56 GHz cryostat will most likely require He filling during operation.

Sextupole-in-Solenoid: Clamping Structure



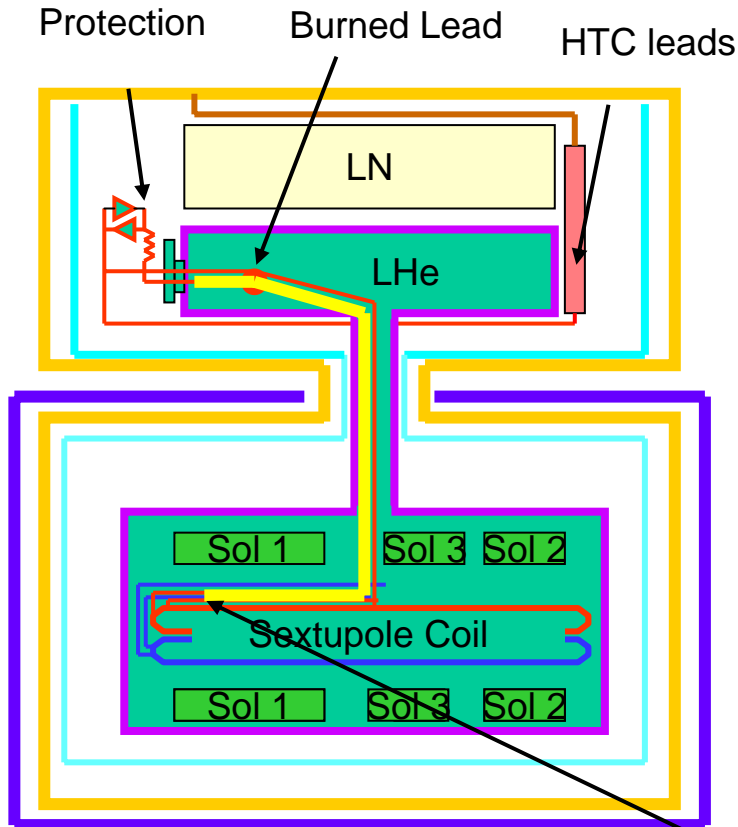
- A shell-based structure using bladders and keys provides a mechanism for controlled room temperature pre-stress.
- Pre-stress is then amplified by the contraction of an aluminum shell during cool-down.
- The method was developed at Superconducting magnet group at LBNL and successfully applied to high field magnets.

- 2D cross section structure analyses has been conducted on the two critical regions
- Stress values are close to the maximum acceptable values
- Needs full 3D analyses



Quench protection

Passive Quench Protection



- Energy stored in the VENUS magnet is 800kJ
- VENUS coils do not require active quench protection
- Leads need protection for adequate cooling
- Energy stored in the 56 GHz Magnet 5.5MJ
- Active Quench protection with heaters at the coils (75% coverage, results in peak temperatures in the coil of 280K)
- Lead protection (Lesson from the VENUS quench failure)

Spliced sextupole lead wire



Other Challenges

- Superconducting Magnet
- Cryogenic Technology
- X-rays from the Plasma
- Ion Beam Transport

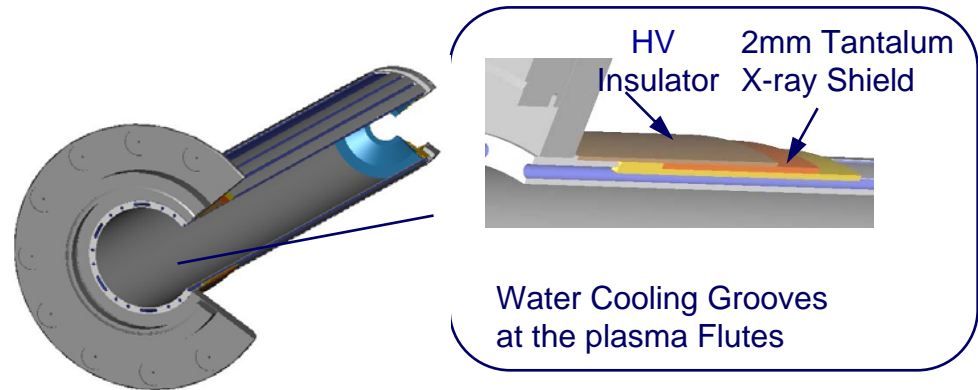
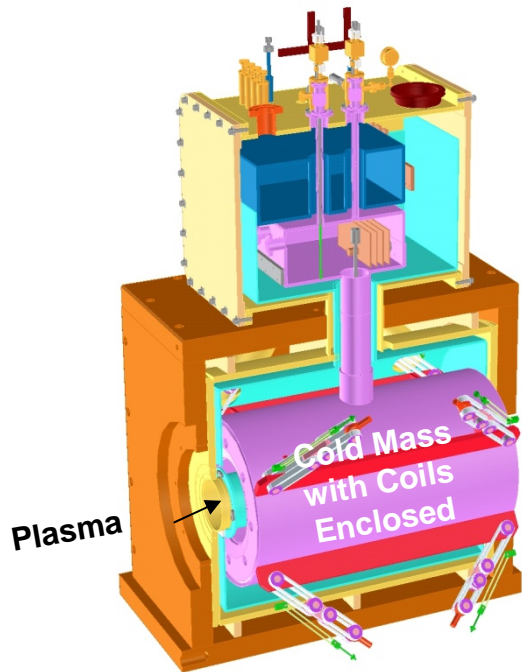




A major challenge for high field SC ECR ion sources is the heat load from bremsstrahlung absorbed in the cryostat

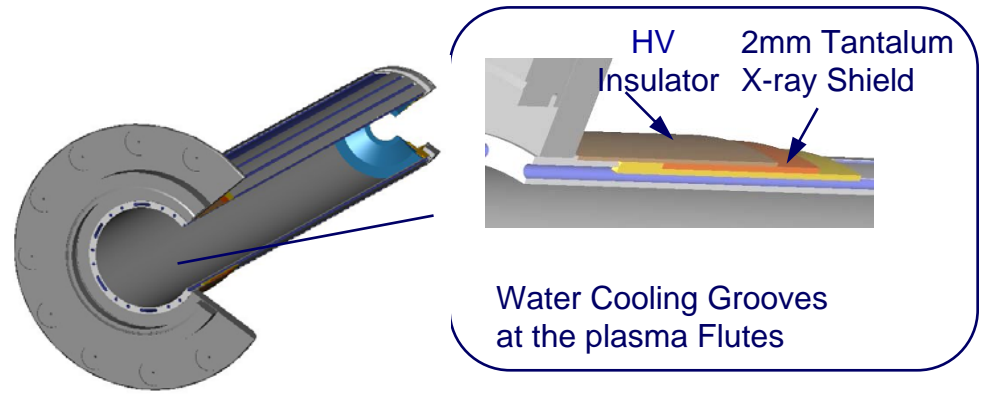
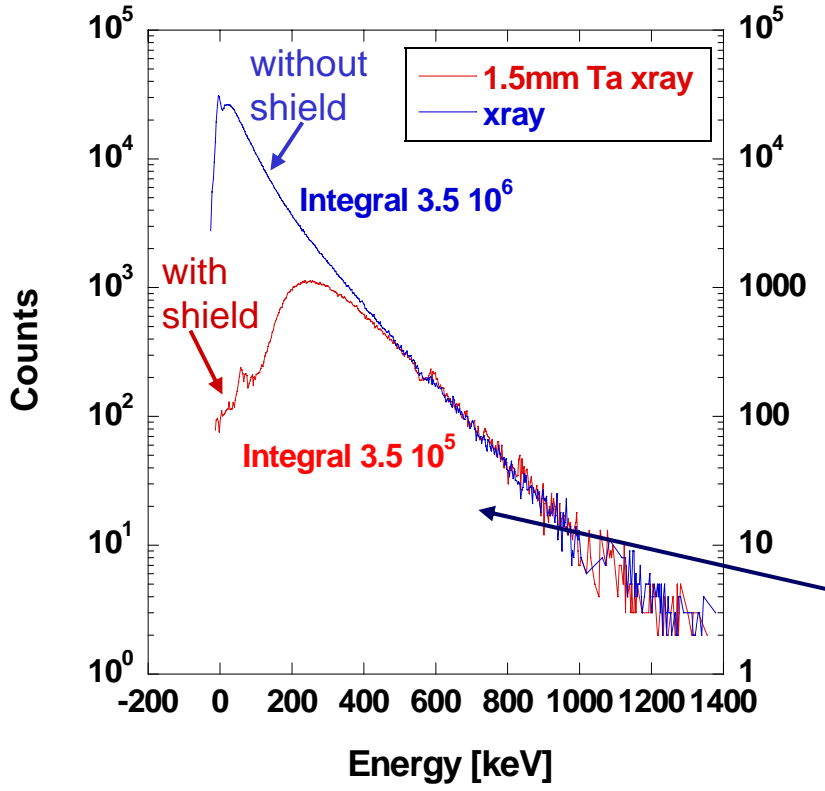
Technical Solution

VENUS Aluminum Plasma Chamber with 2mm Ta x-ray shield





A major challenge for high field SC ECR ion sources is the heat load from bremsstrahlung absorbed in the cryostat

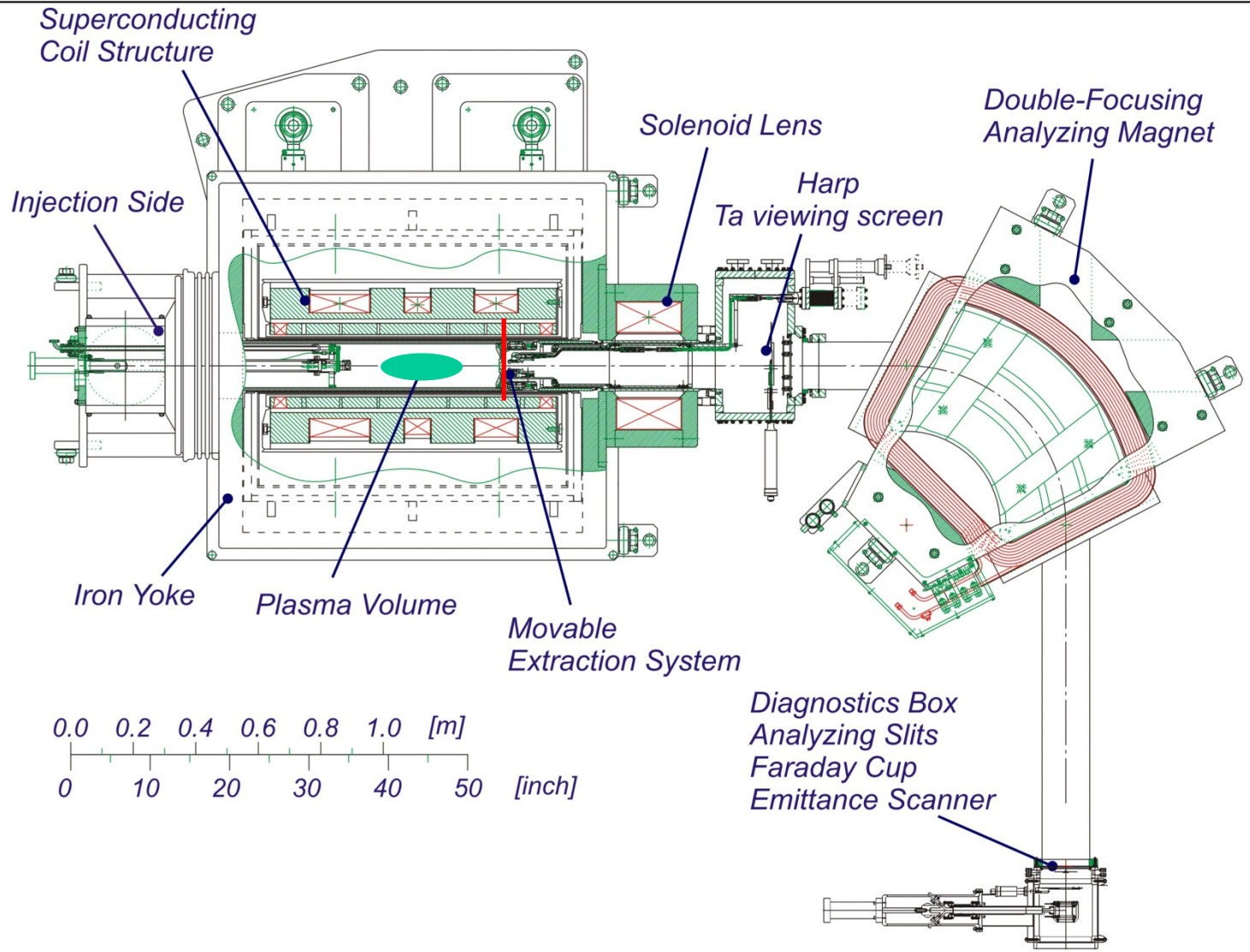


1.5 - 2 mm Ta shielding effectively attenuates the low energy bremsstrahlung, but becomes transparent for x-rays above 400keV

The high energy tail of the x-ray spectrum increases substantially at the higher microwave frequency (10s of) watts of cooling power must be reserved for the cryostat.

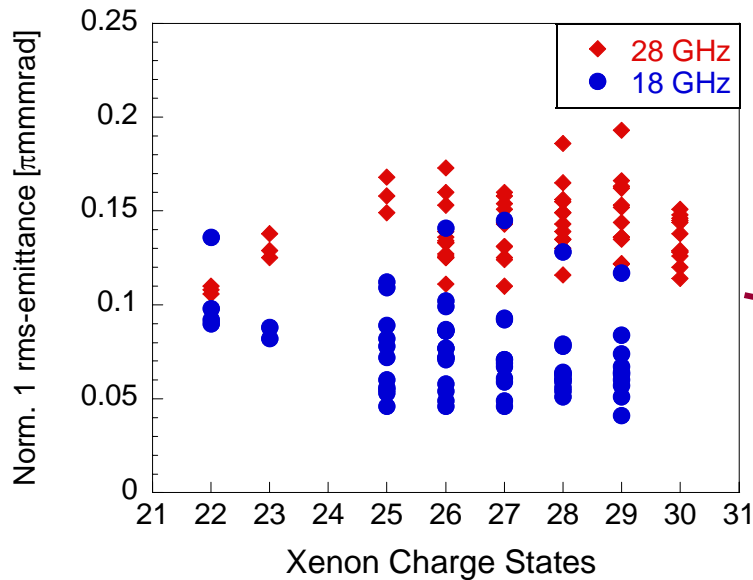
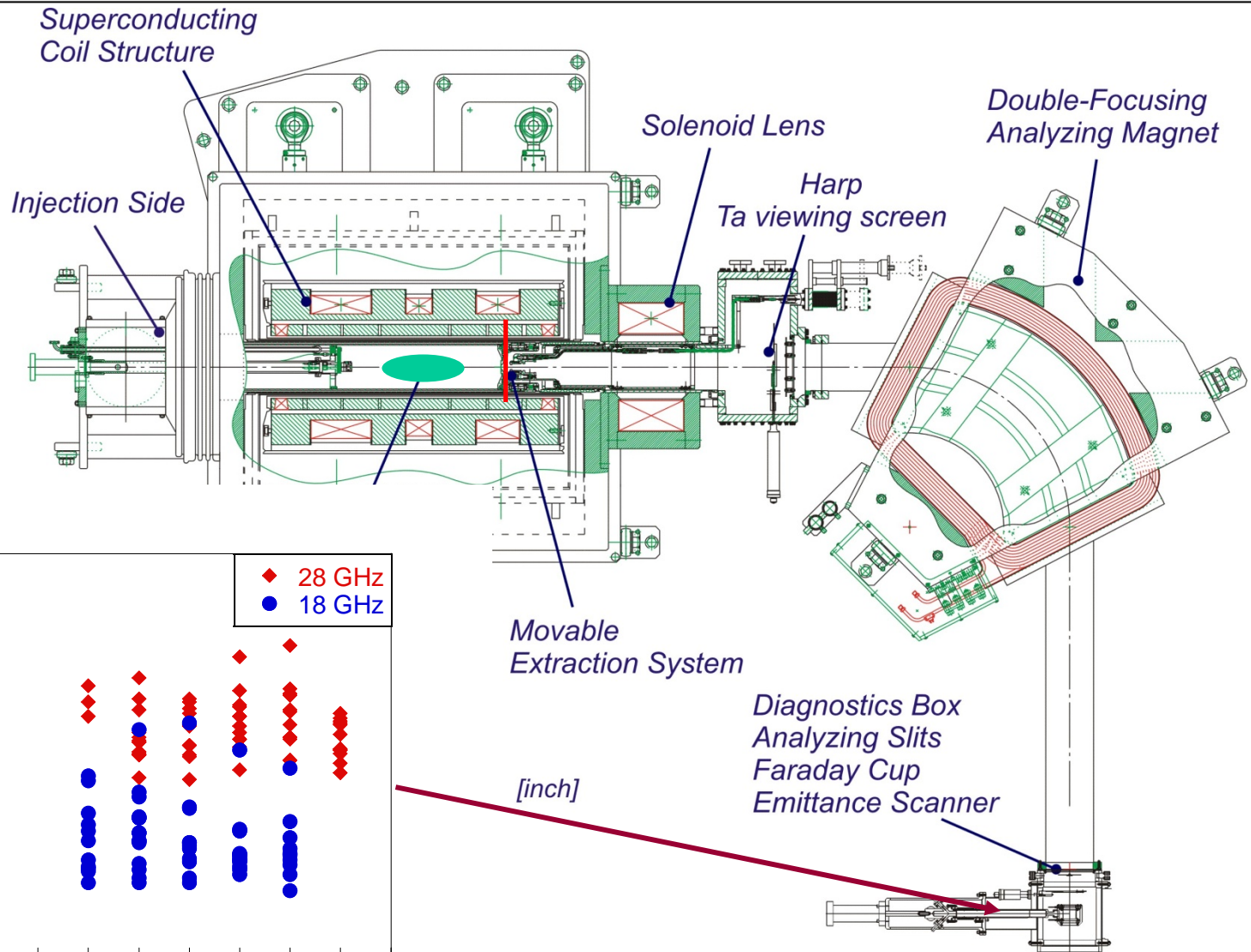


Beam transport is a challenge for high field SC ECR ion sources





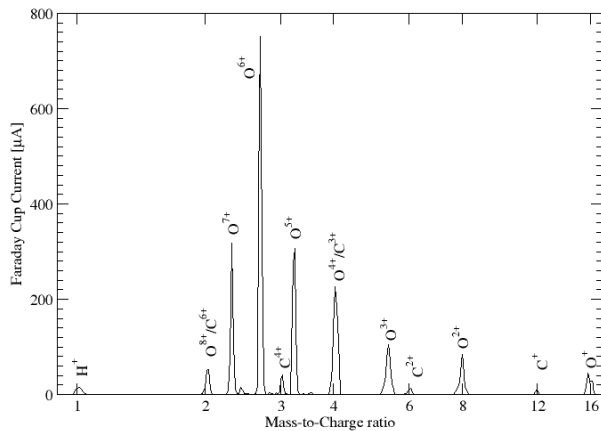
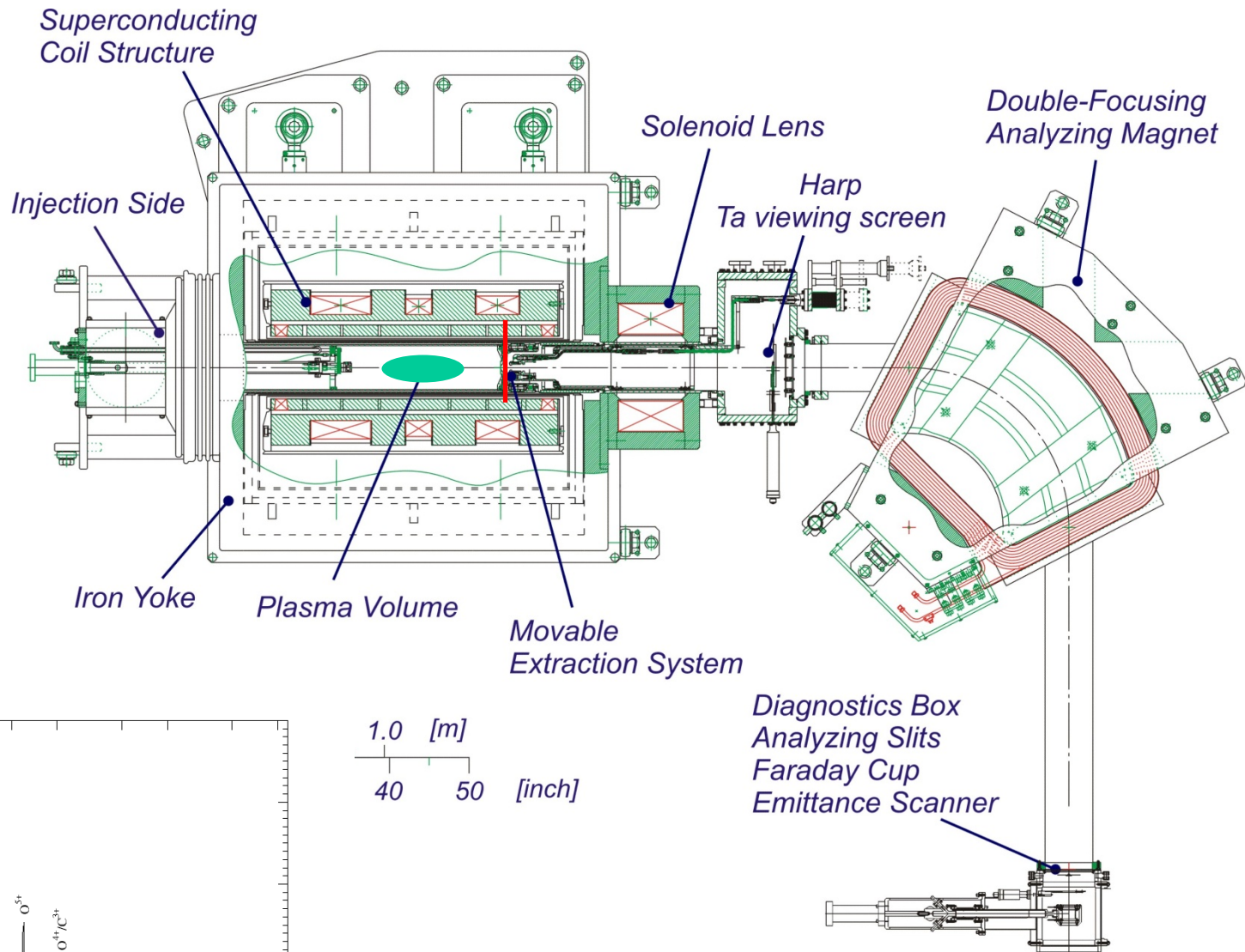
Beam transport is a challenge for high field SC ECR ion sources



Beam emittance grows with magnetic field at extraction (therefore with heating frequency)



Beam transport is a challenge for high field SC ECR ion sources

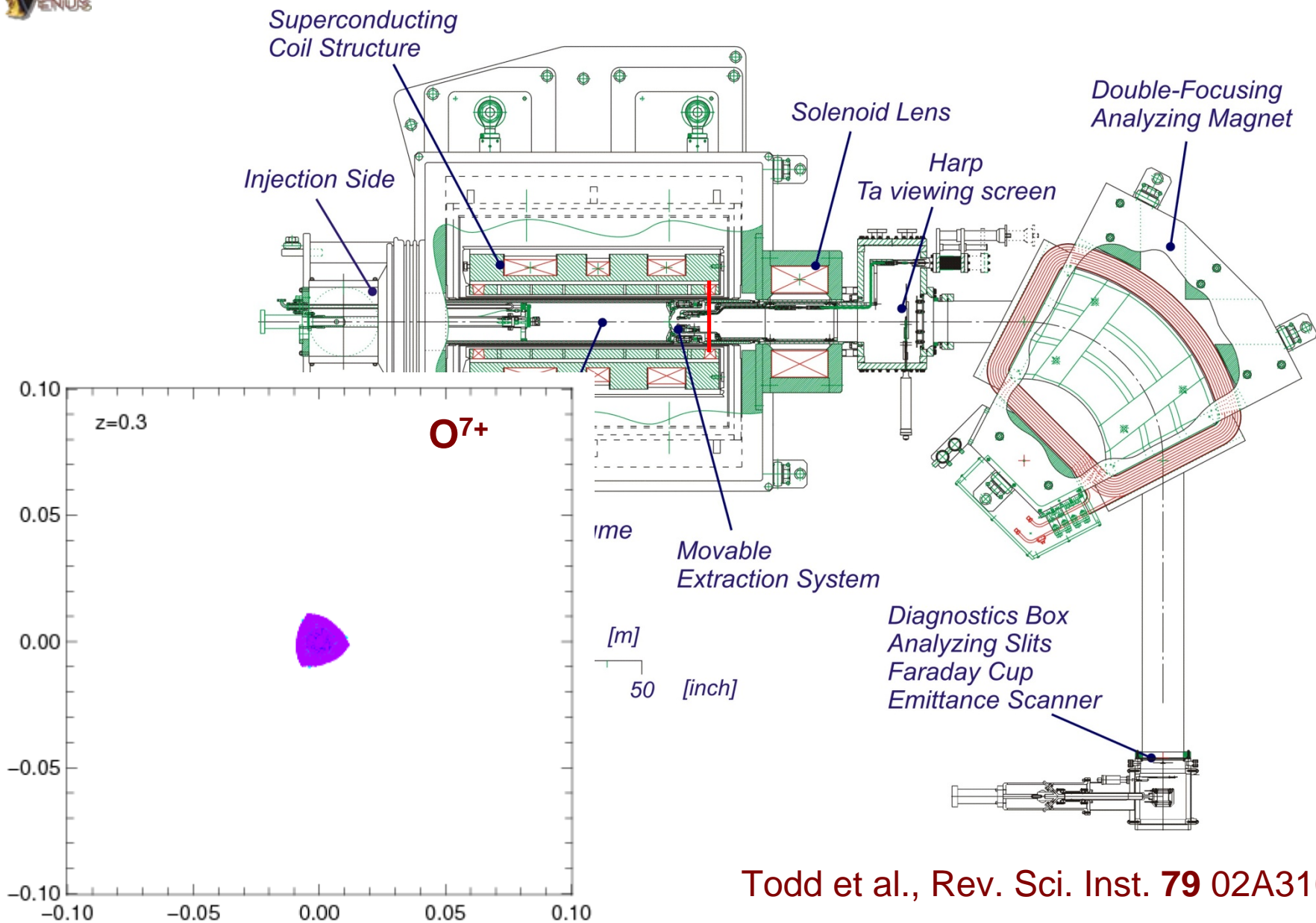


1.0 [m]
40 50 [inch]

Todd et al., Rev. Sci. Inst. **79** 02A316



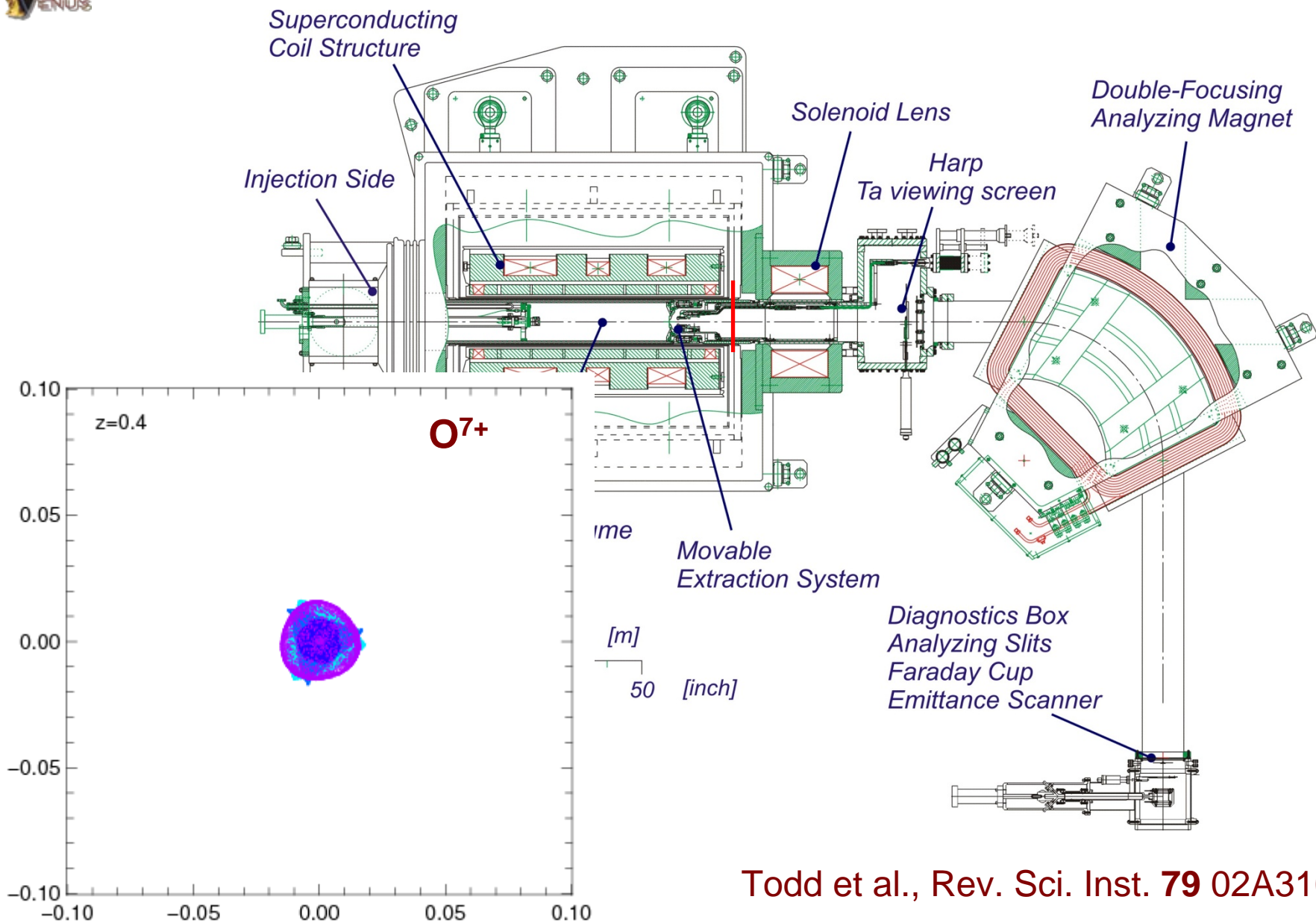
Simulation of oxygen beam extraction and transport



Todd et al., Rev. Sci. Inst. **79** 02A316



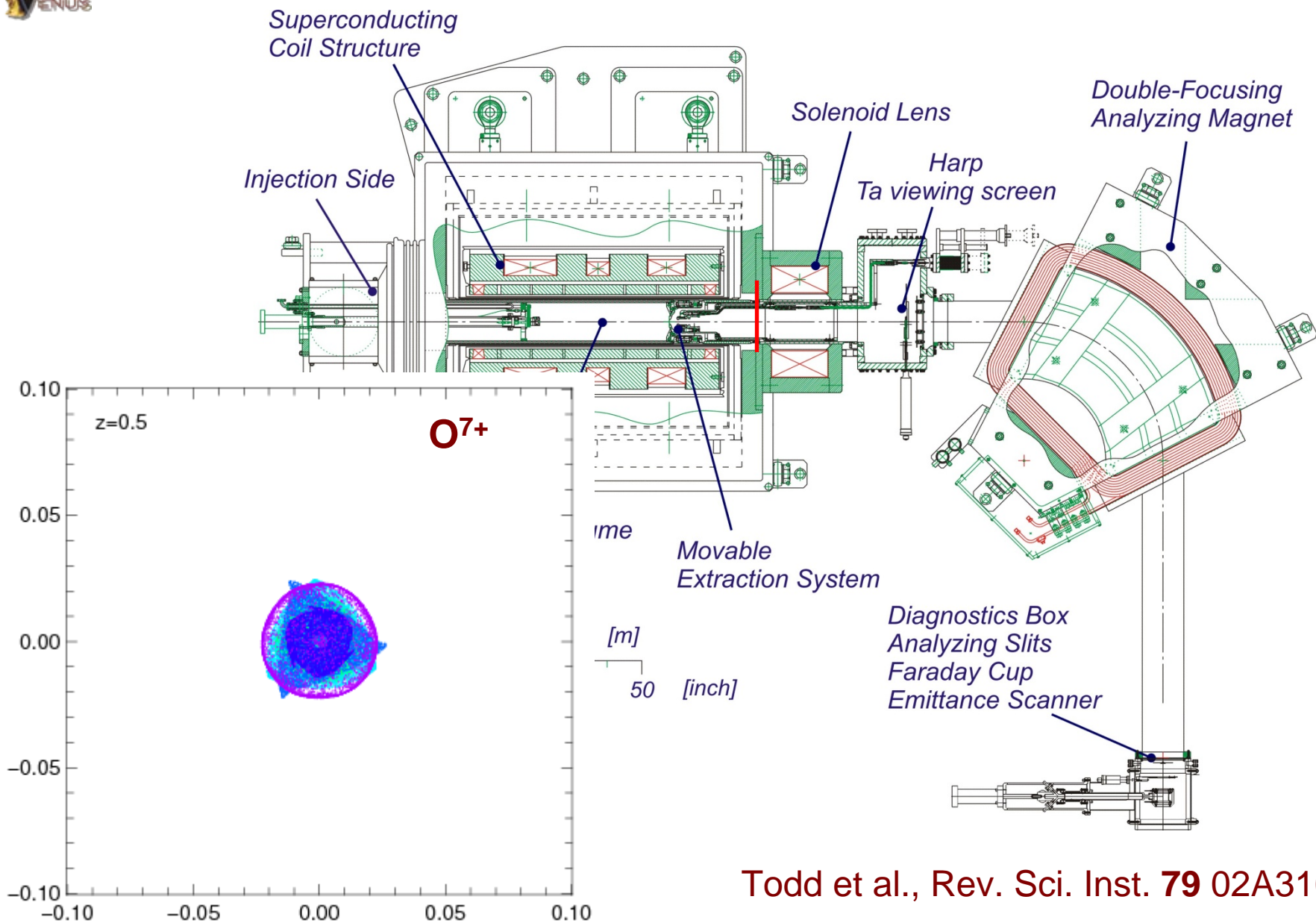
Simulation of oxygen beam extraction and transport



Todd et al., Rev. Sci. Inst. **79** 02A316



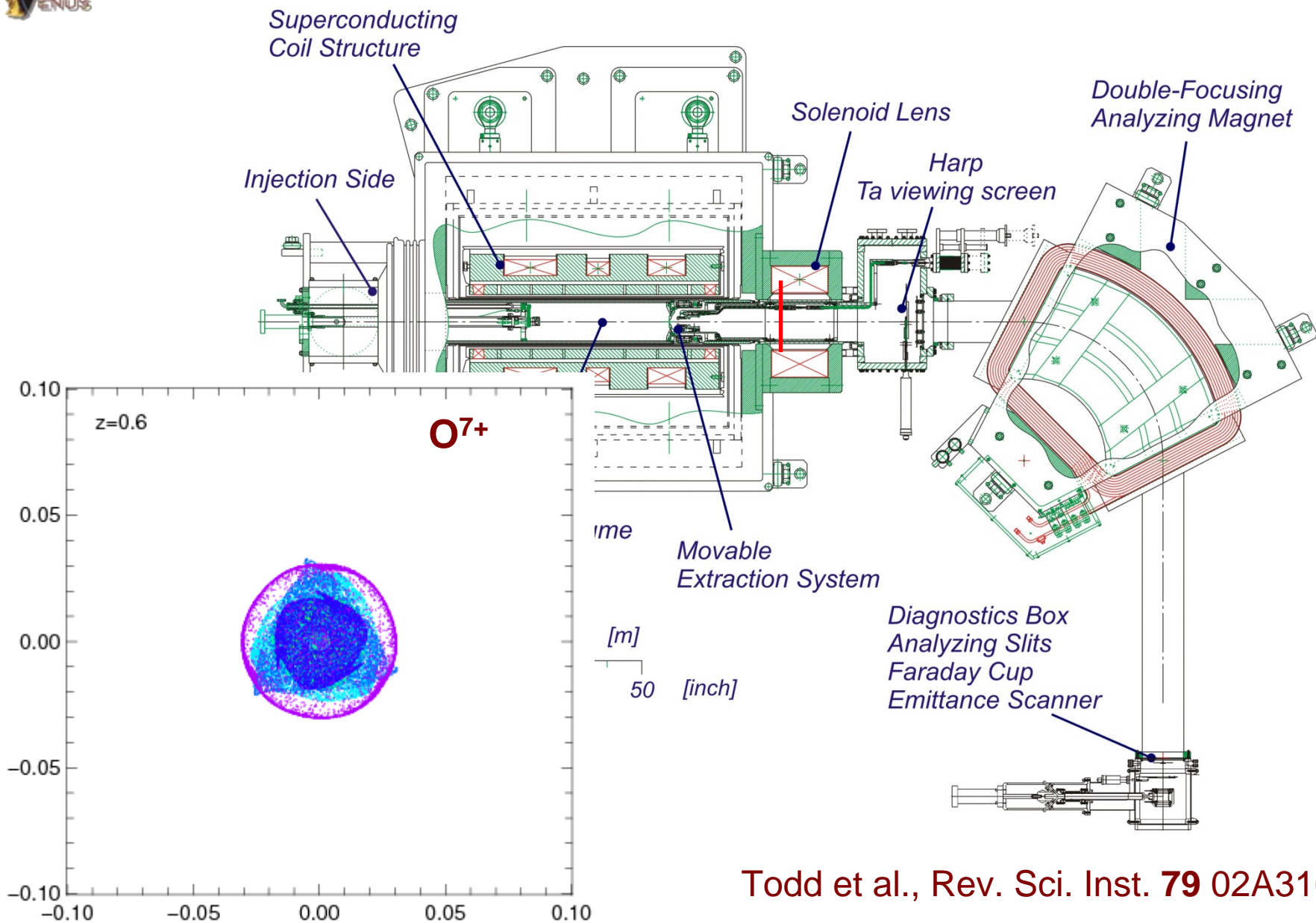
Simulation of oxygen beam extraction and transport



Todd et al., Rev. Sci. Inst. **79** 02A316



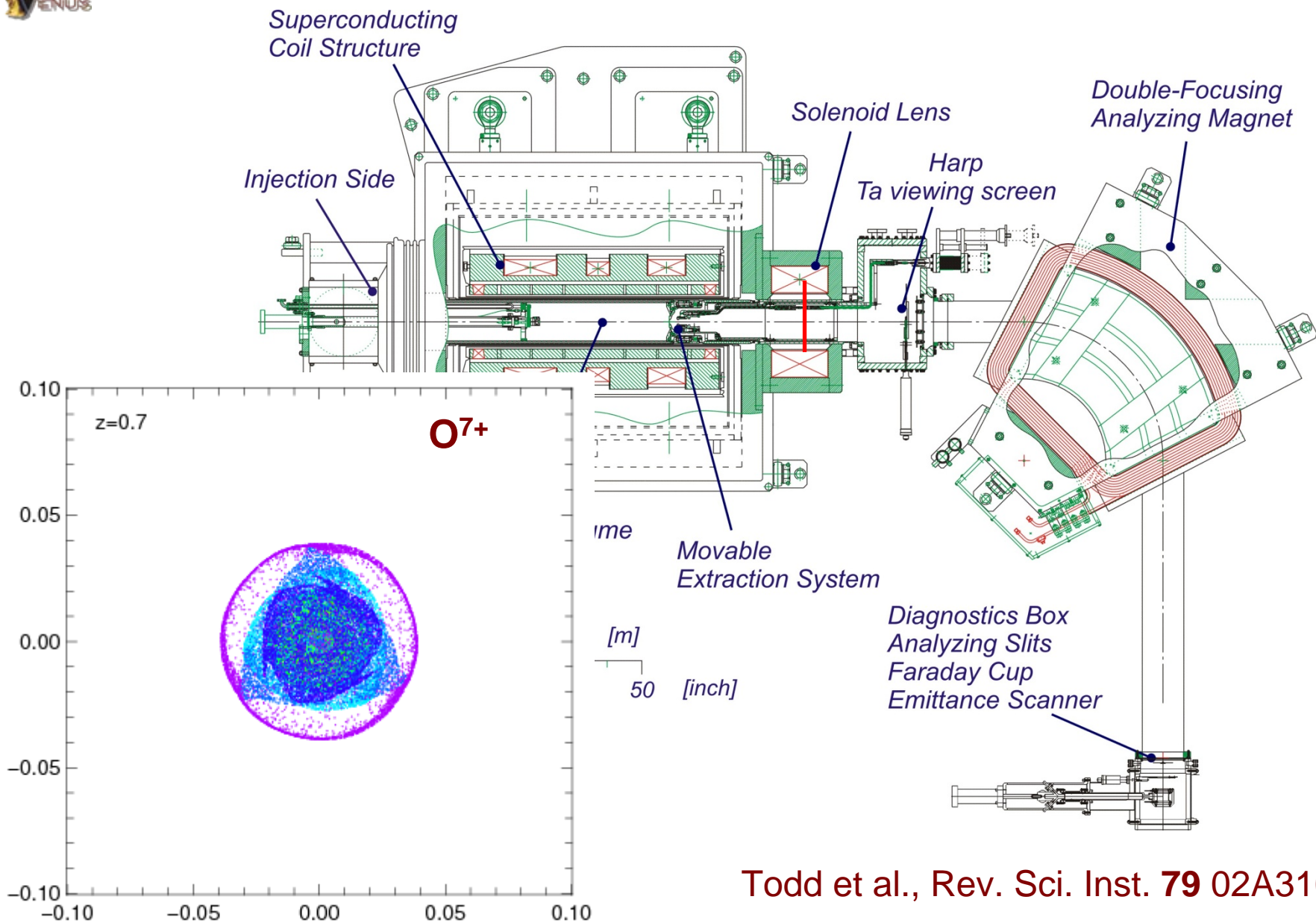
Simulation of oxygen beam extraction and transport



Todd et al., Rev. Sci. Inst. **79** 02A316

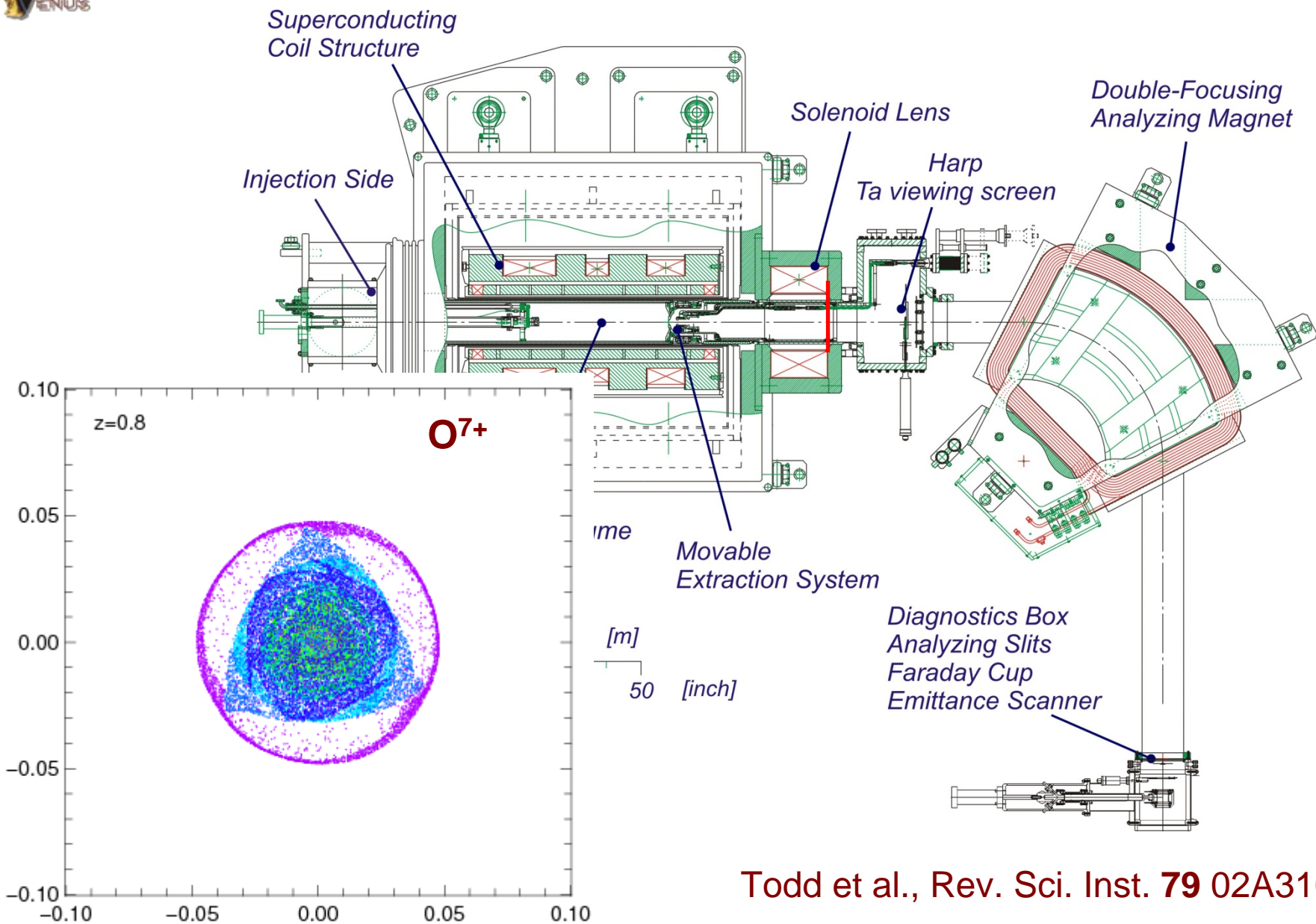


Simulation of oxygen beam extraction and transport



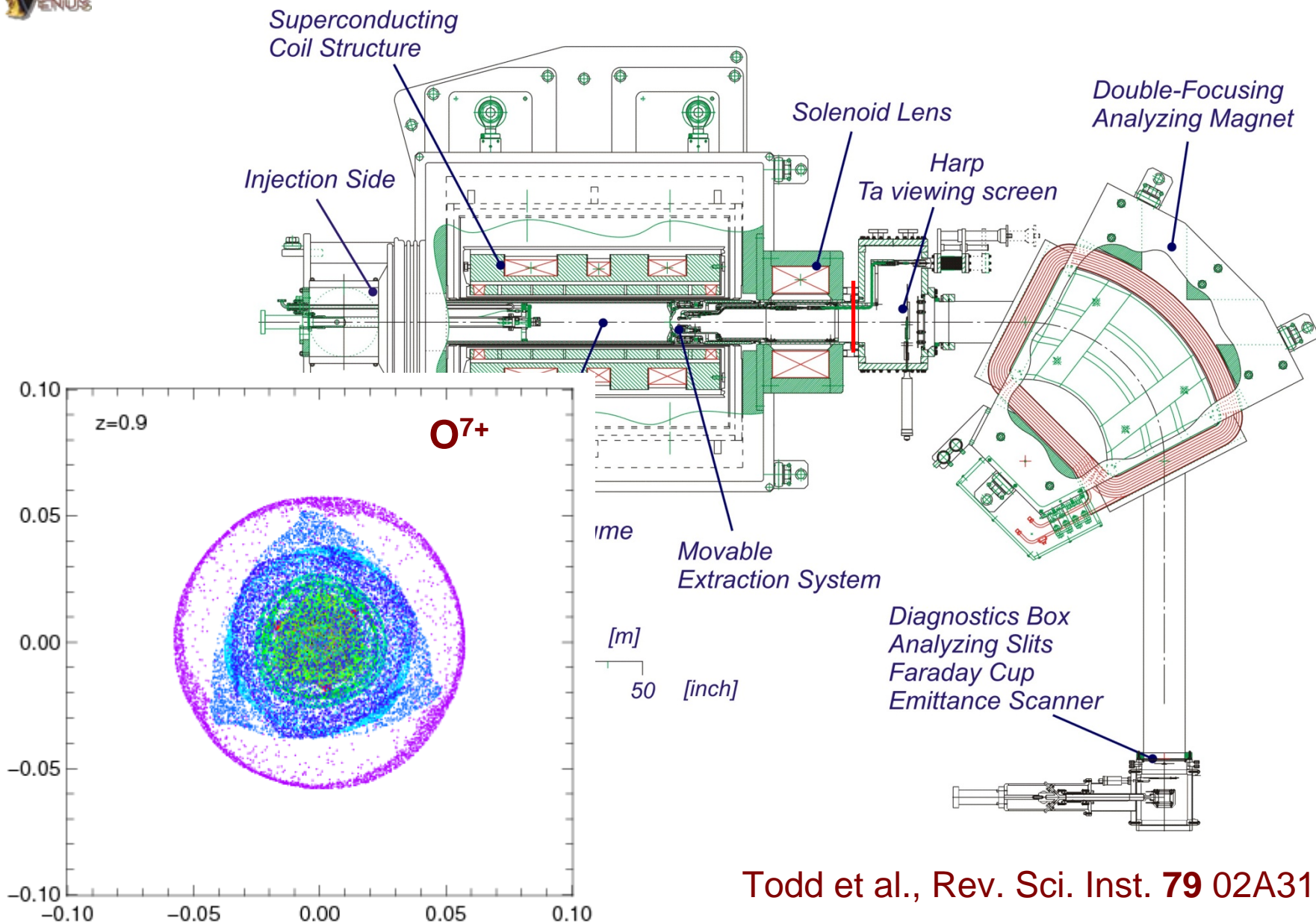


Simulation of oxygen beam extraction and transport



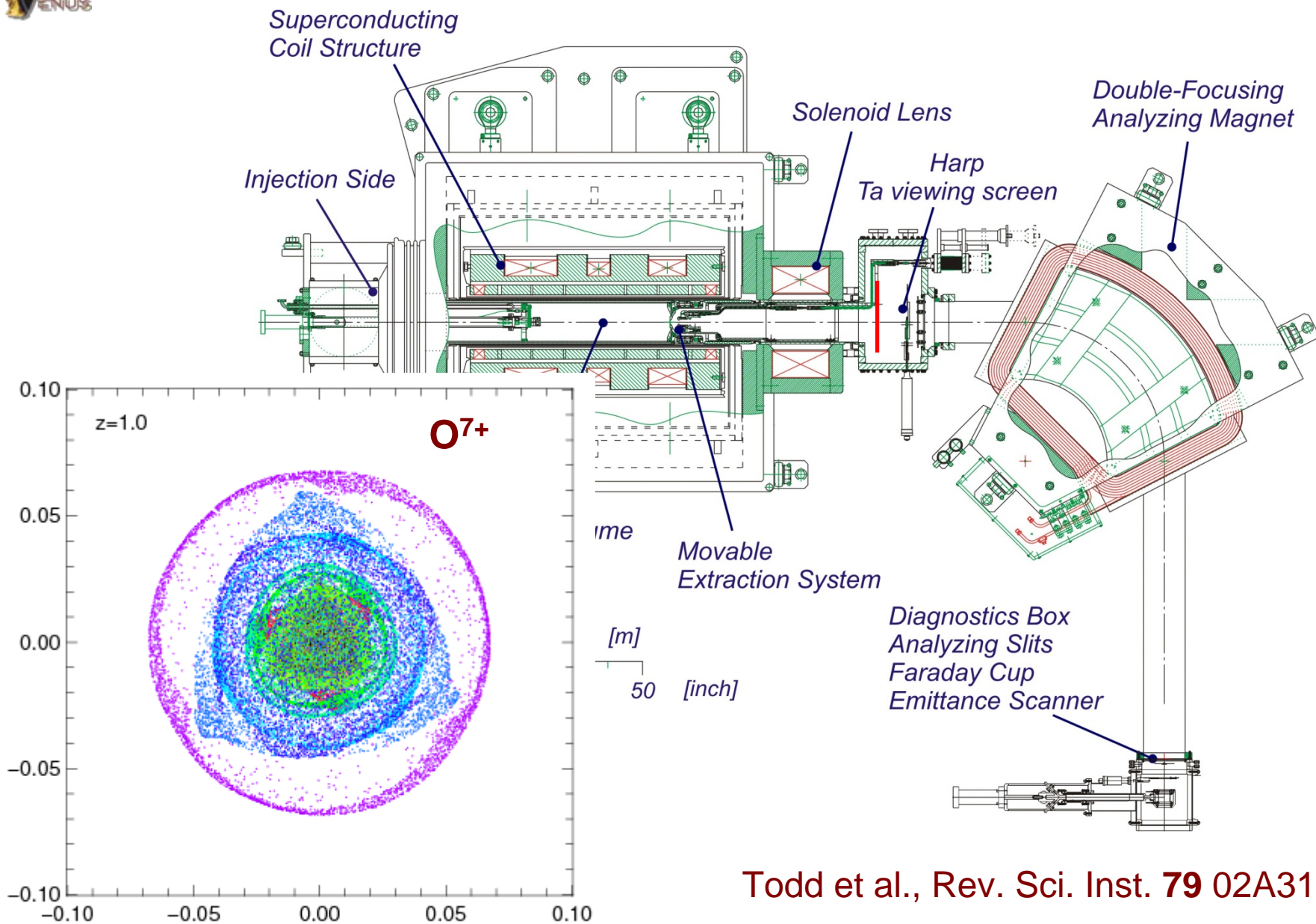


Simulation of oxygen beam extraction and transport





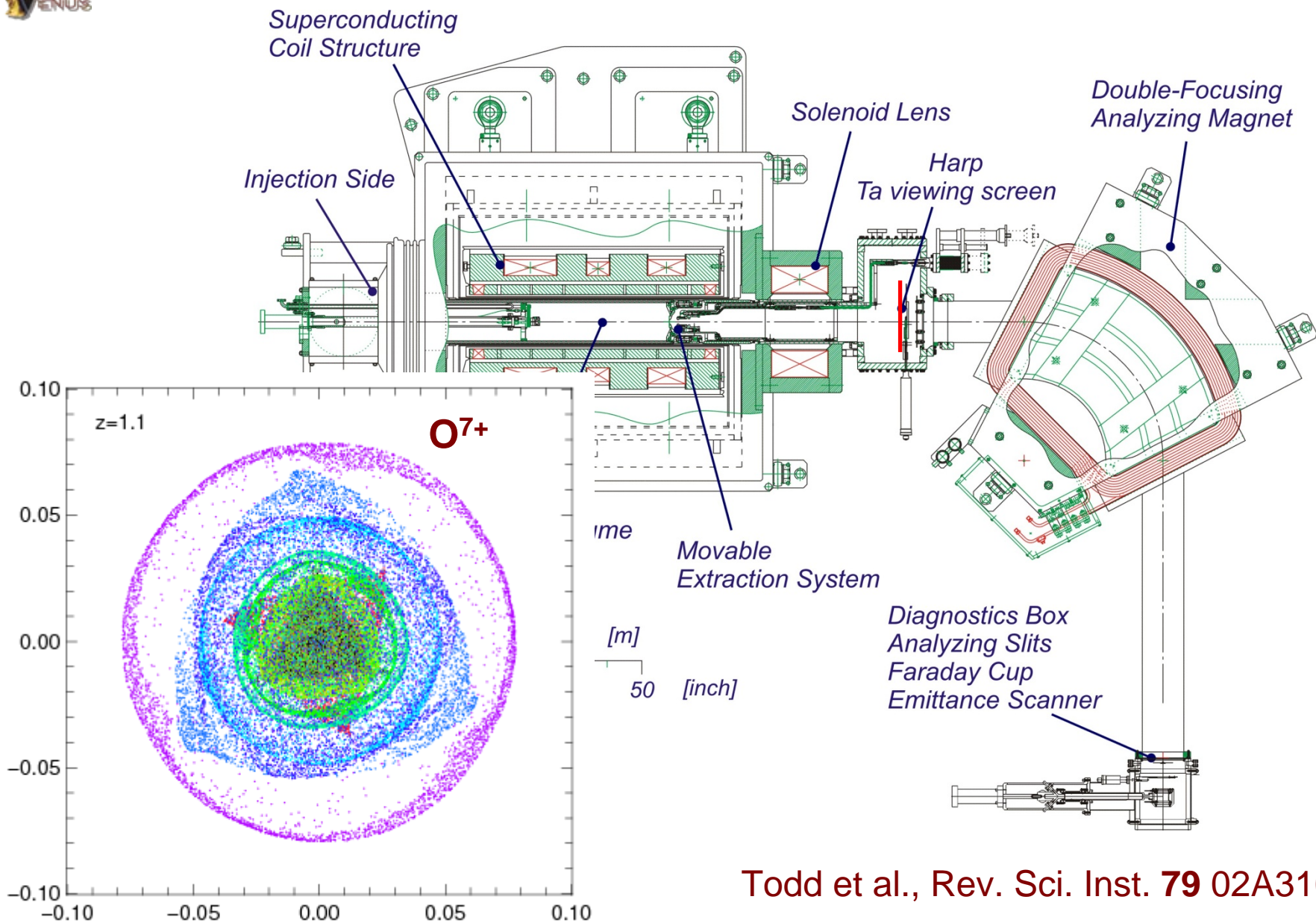
Simulation of oxygen beam extraction and transport



Todd et al., Rev. Sci. Inst. **79** 02A316



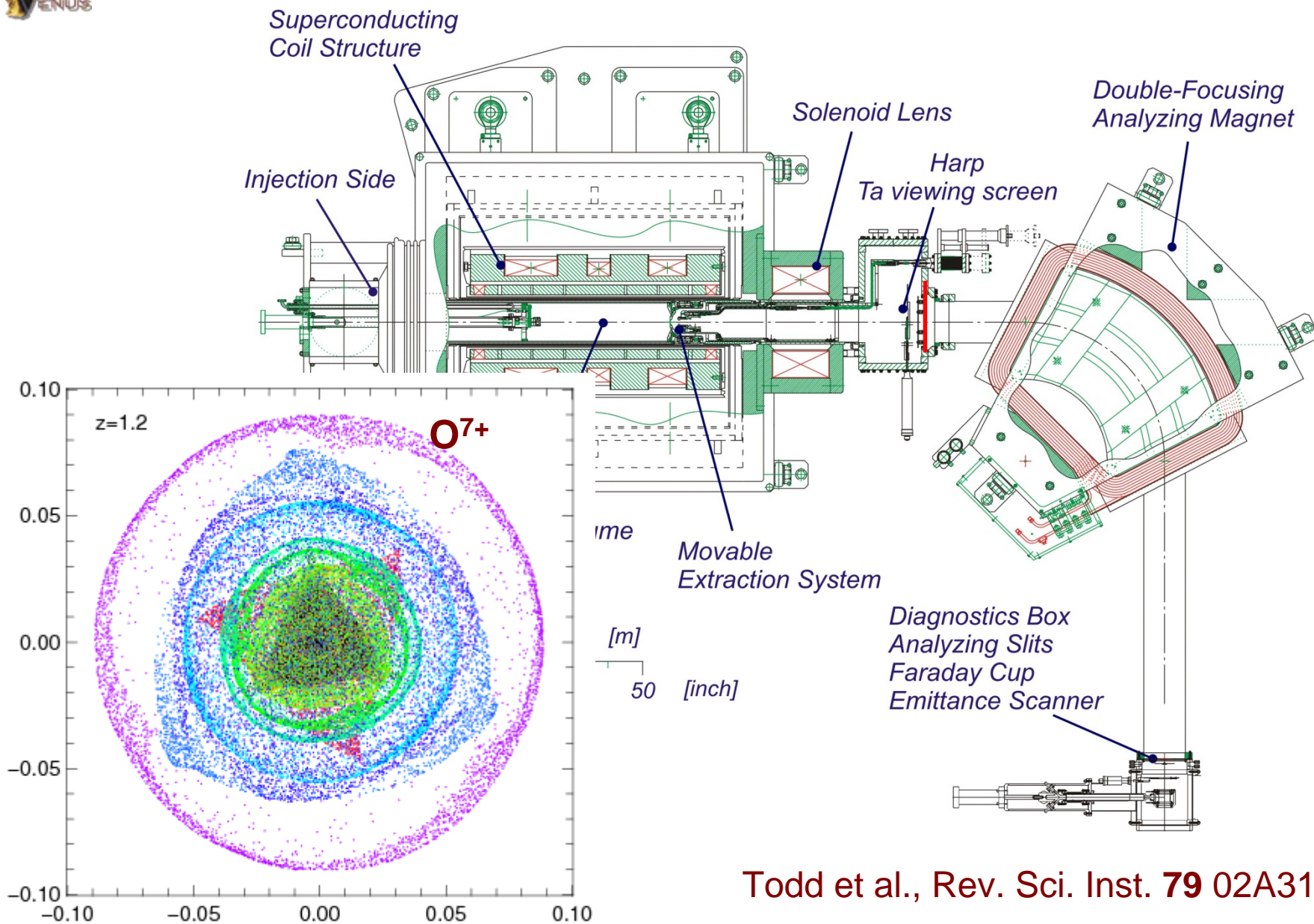
Simulation of oxygen beam extraction and transport



Todd et al., Rev. Sci. Inst. **79** 02A316

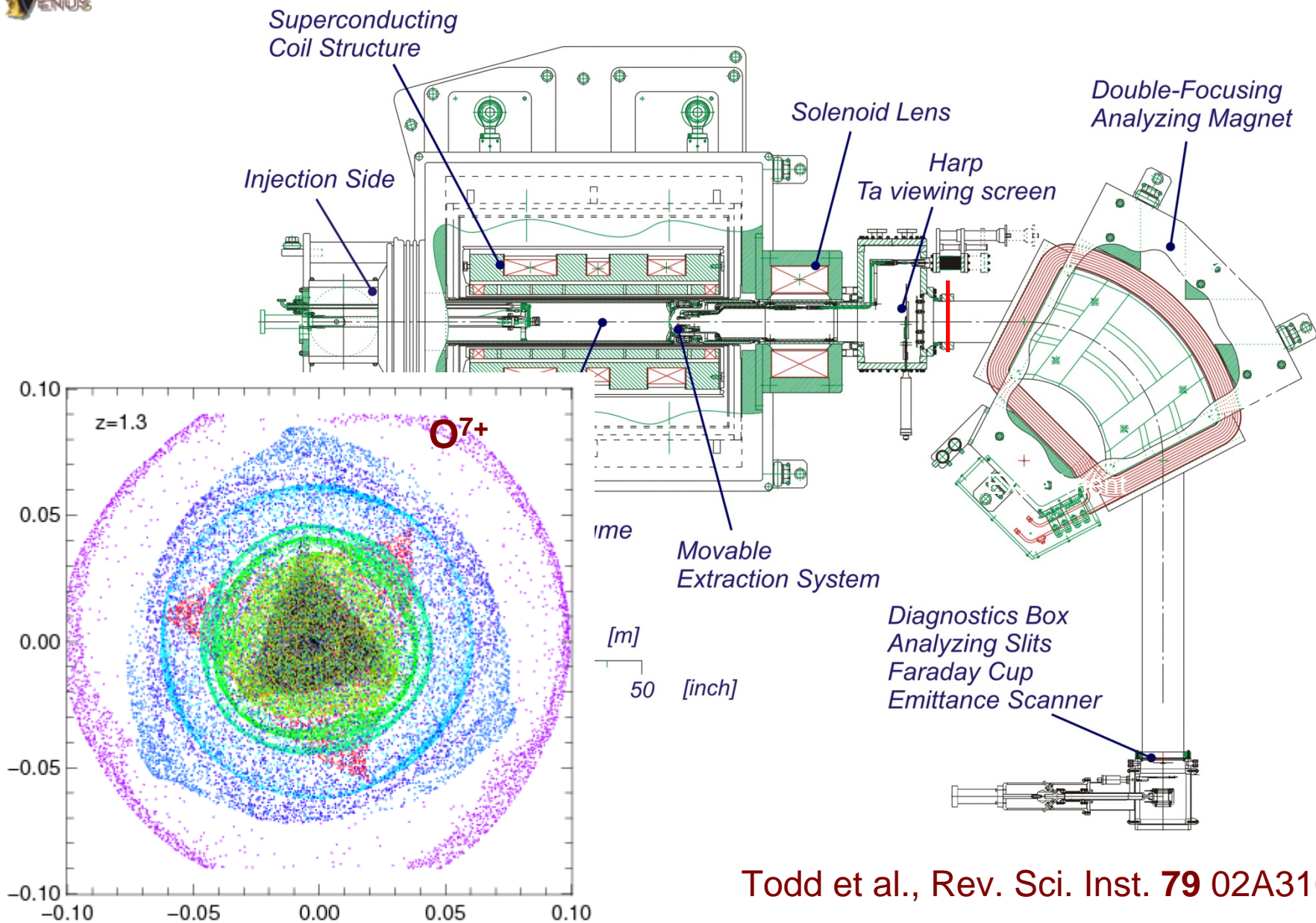


Simulation of oxygen beam extraction and transport





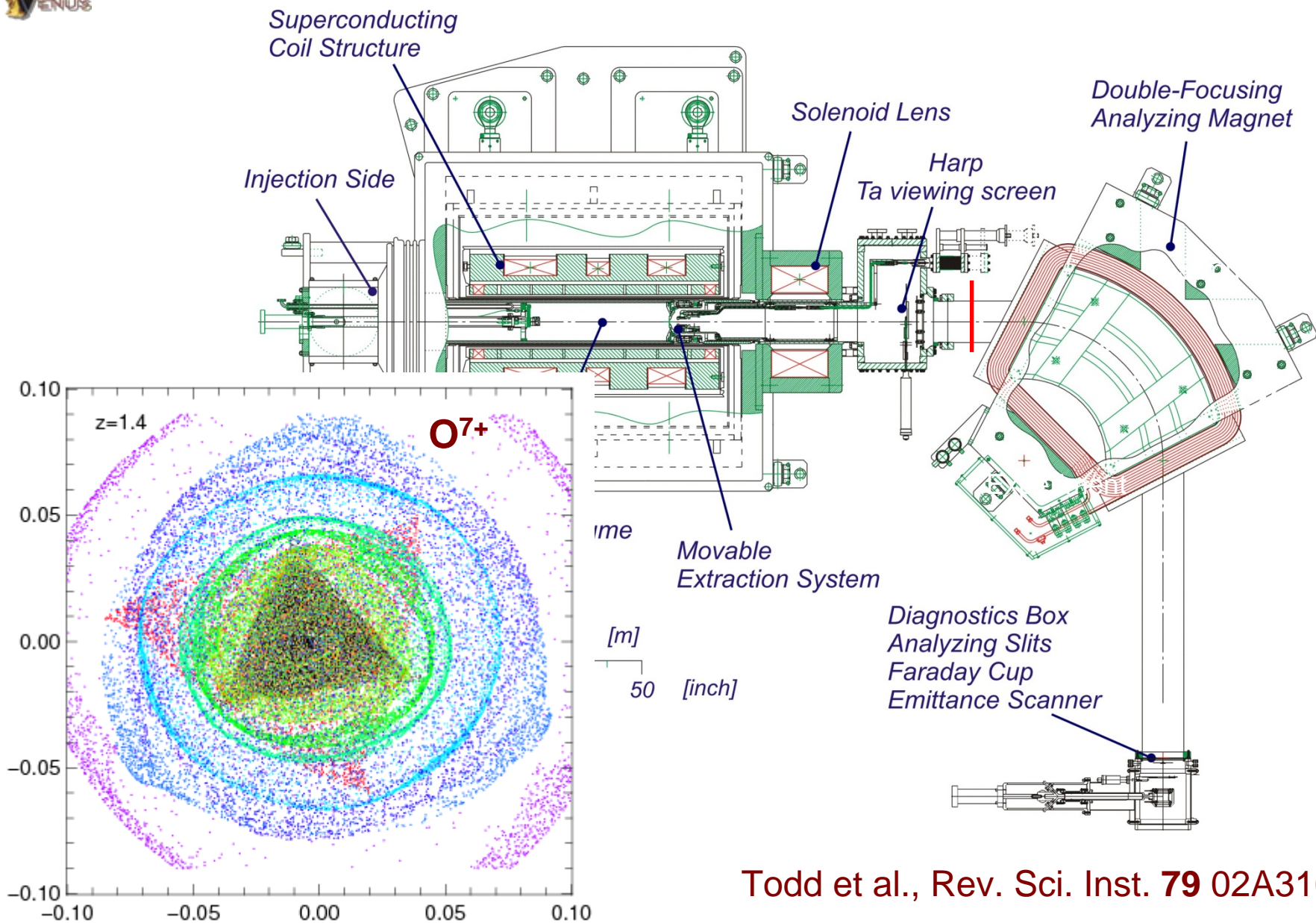
Simulation of oxygen beam extraction and transport



Todd et al., Rev. Sci. Inst. **79** 02A316



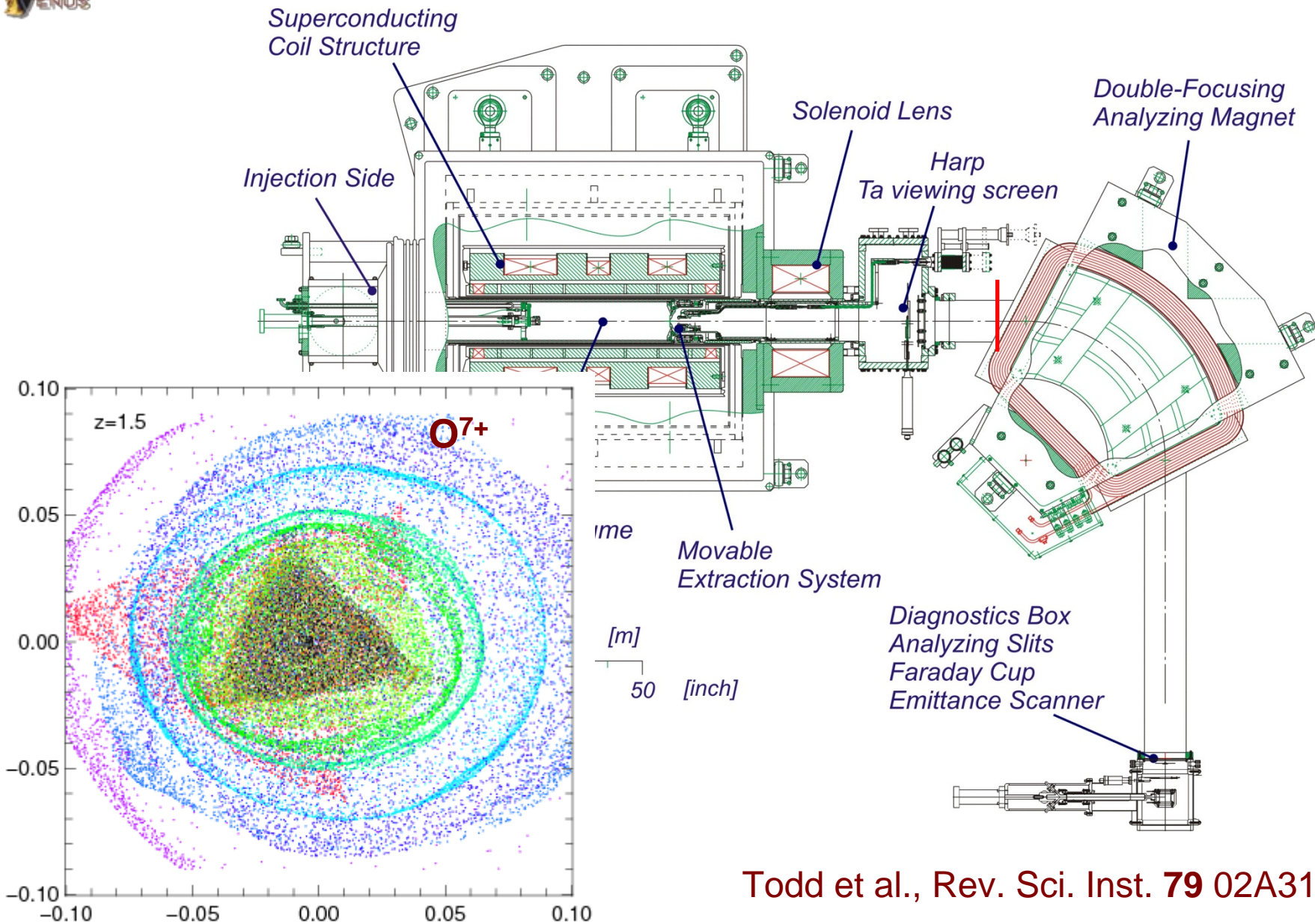
Simulation of oxygen beam extraction and transport



Todd et al., Rev. Sci. Inst. **79** 02A316

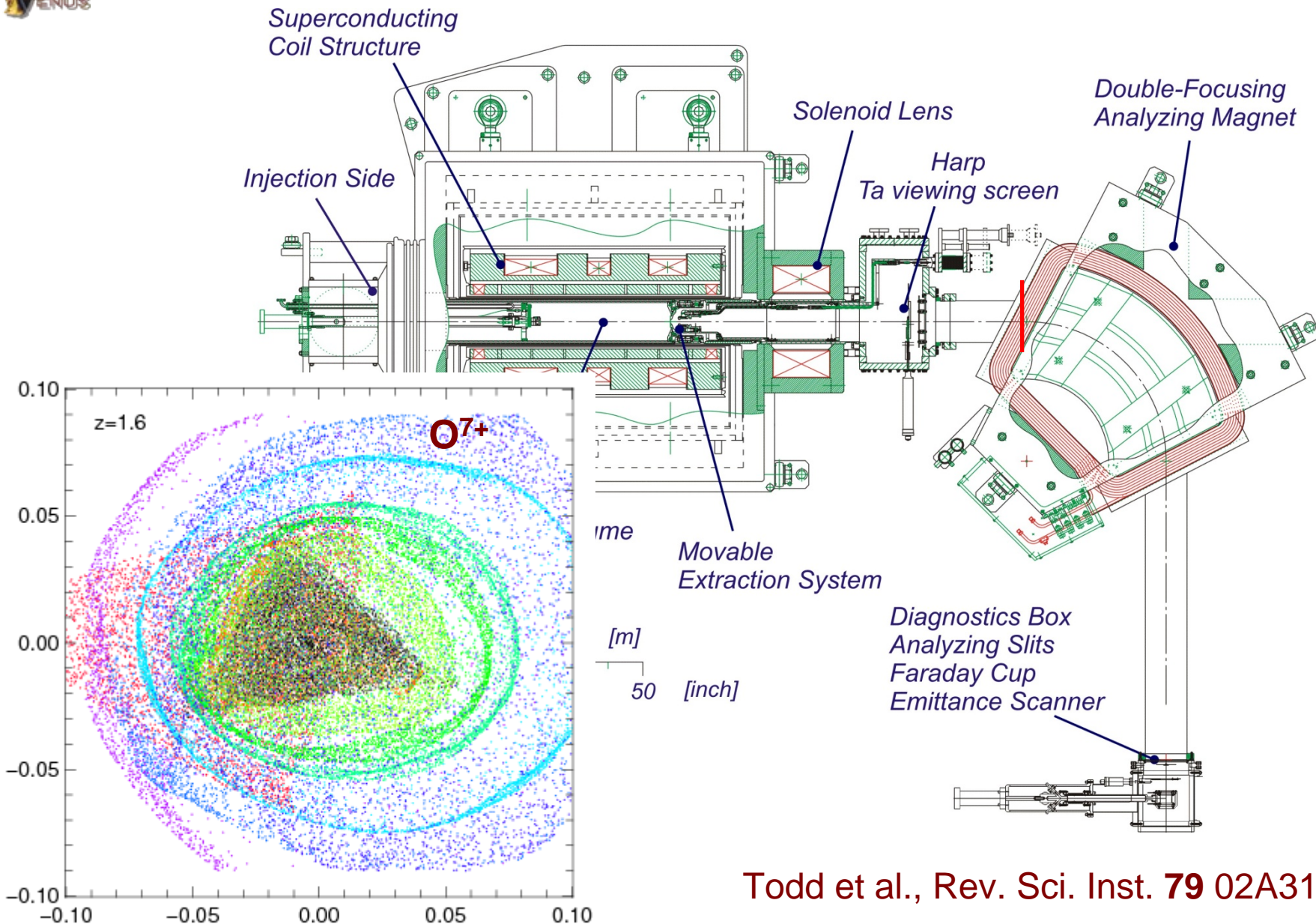


Simulation of oxygen beam extraction and transport





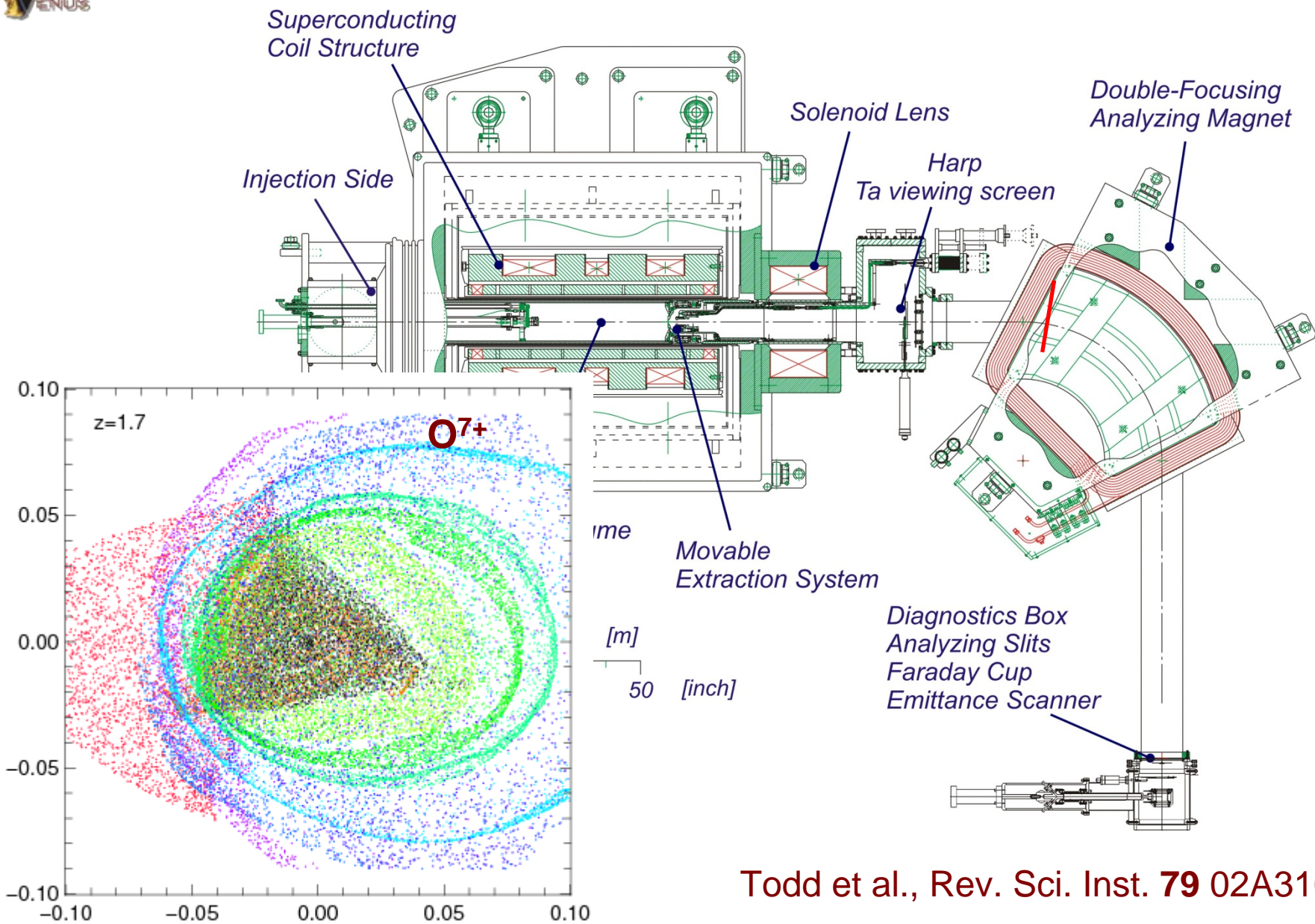
Simulation of oxygen beam extraction and transport



Todd et al., Rev. Sci. Inst. **79** 02A316

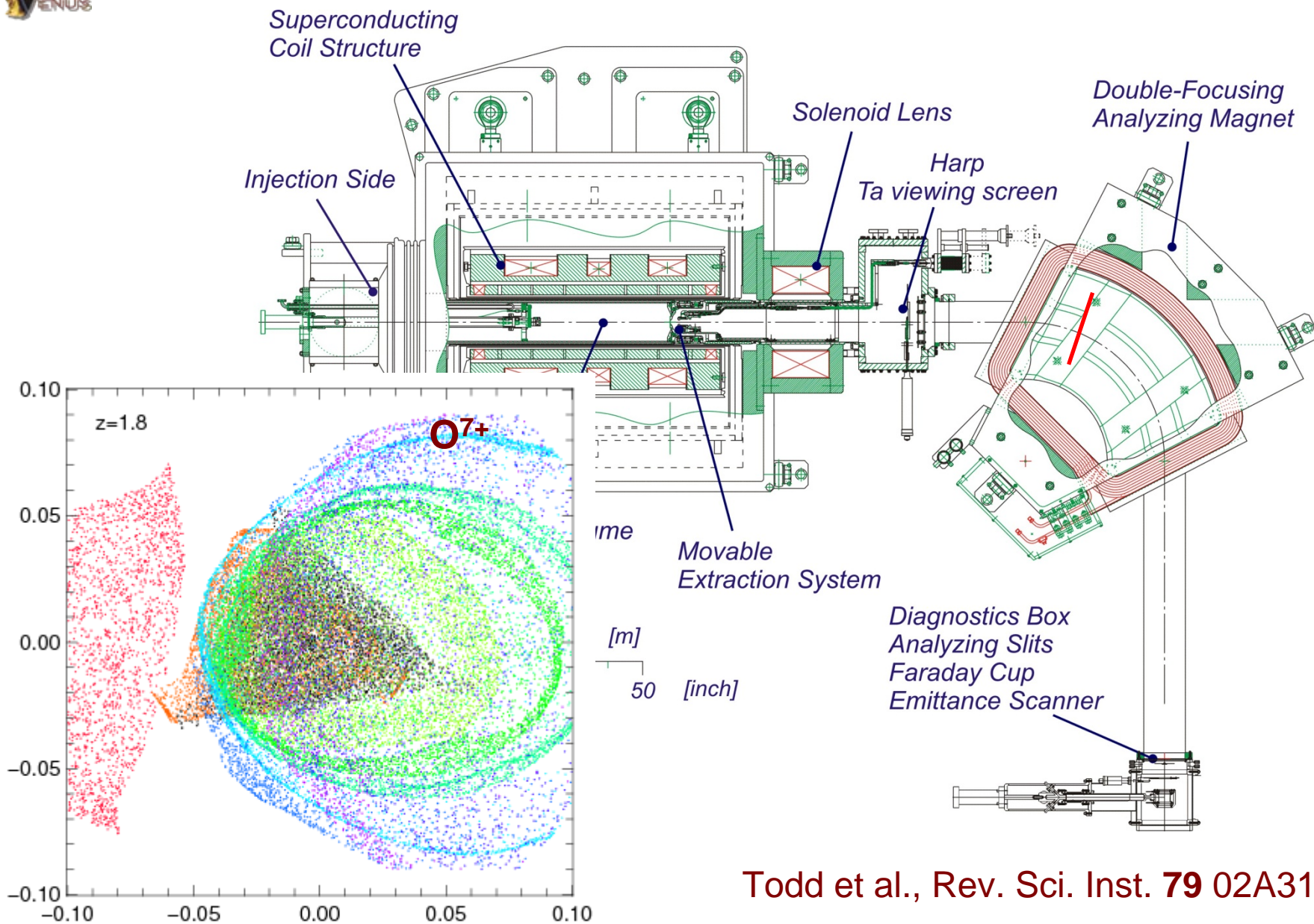


Simulation of oxygen beam extraction and transport





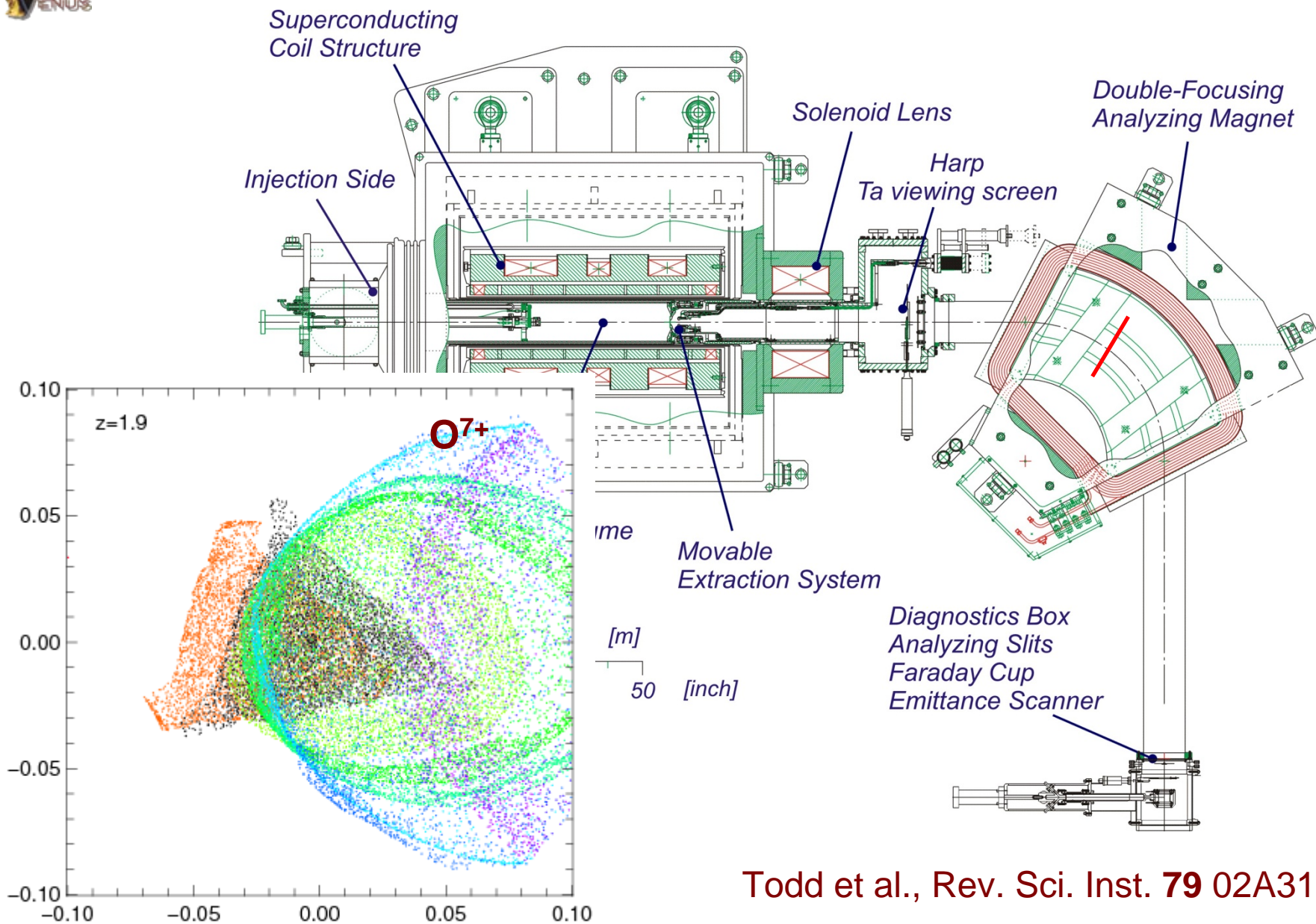
Simulation of oxygen beam extraction and transport



Todd et al., Rev. Sci. Inst. **79** 02A316



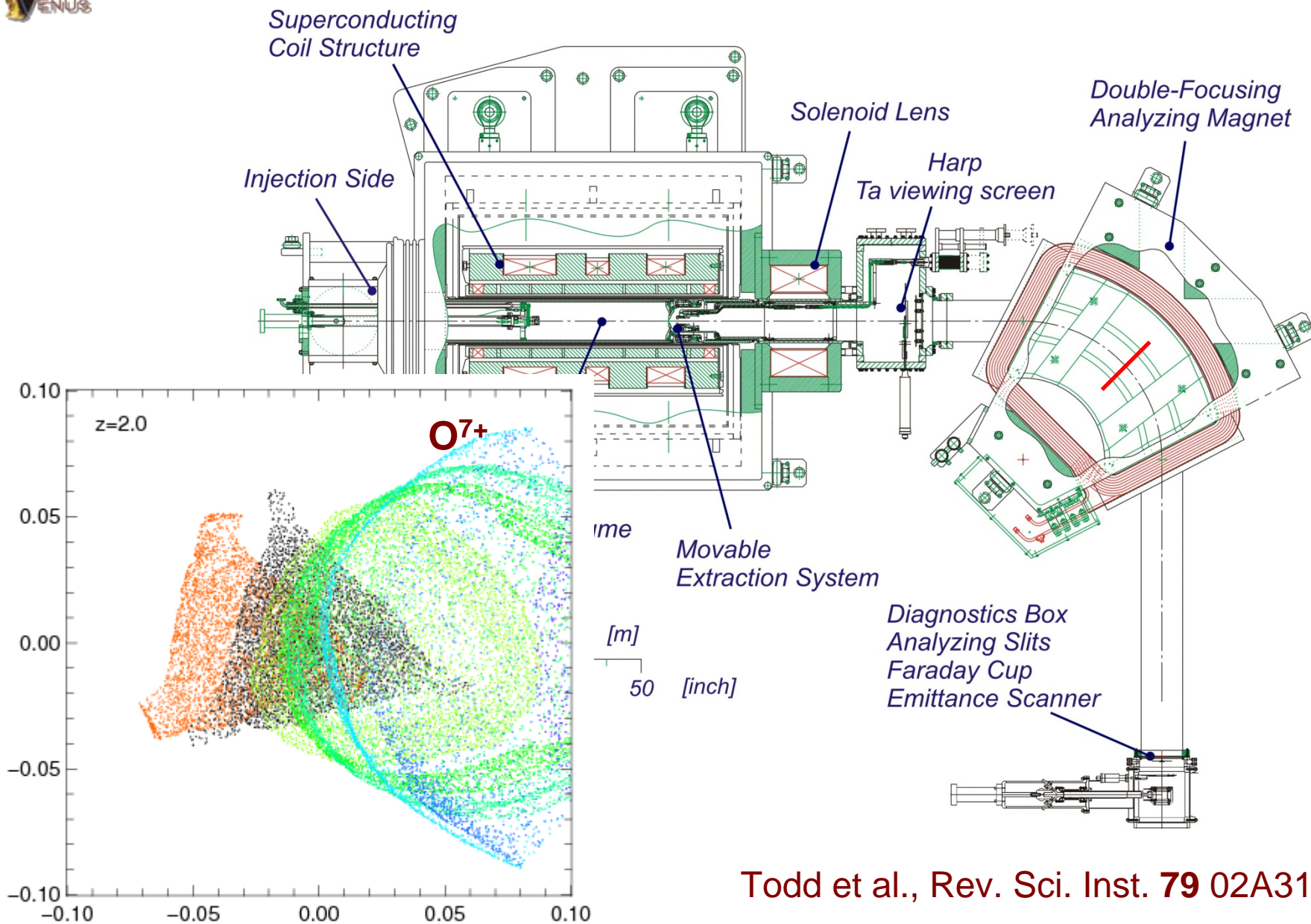
Simulation of oxygen beam extraction and transport



Todd et al., Rev. Sci. Inst. **79** 02A316



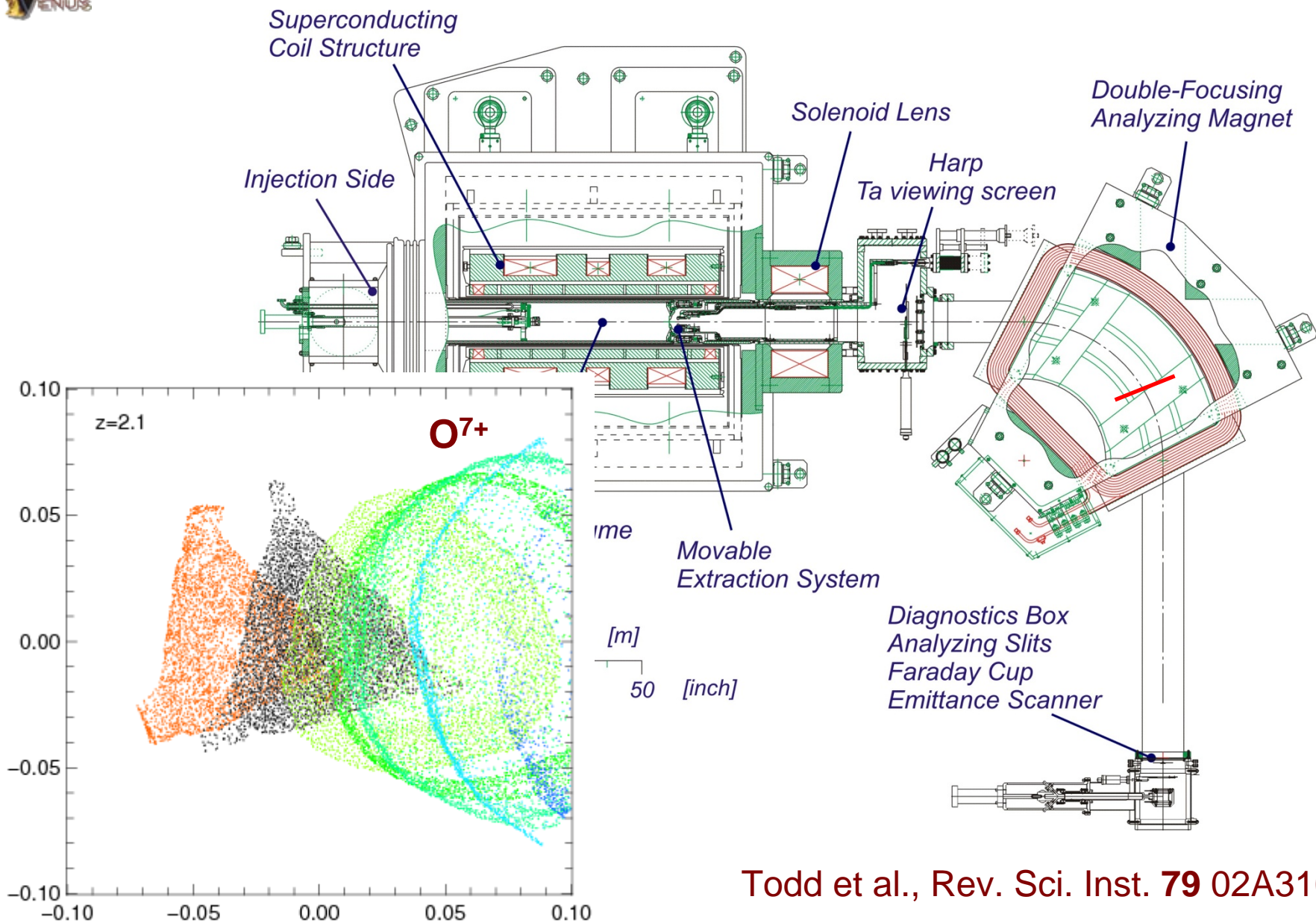
Simulation of oxygen beam extraction and transport



Todd et al., Rev. Sci. Inst. **79** 02A316



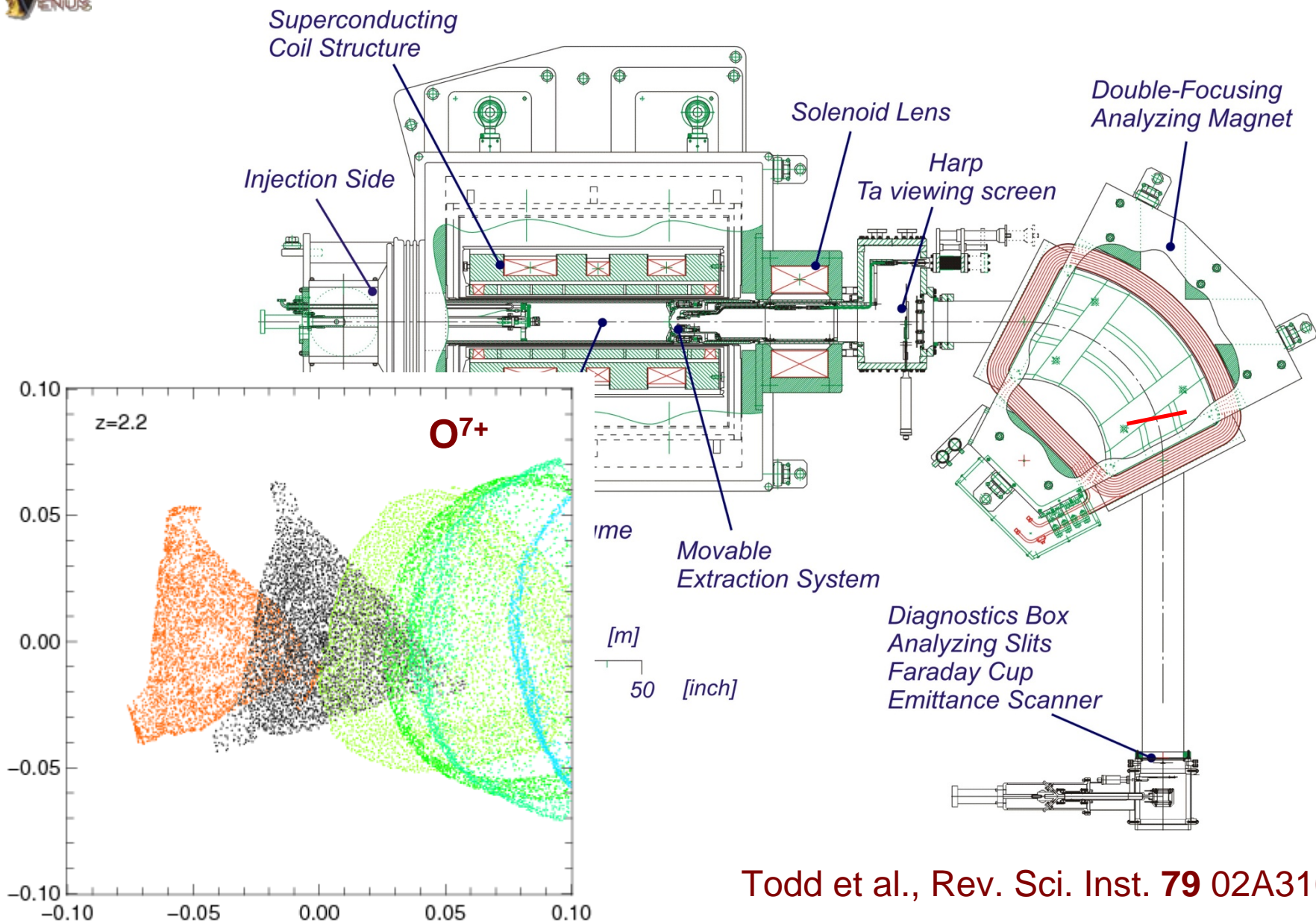
Simulation of oxygen beam extraction and transport



Todd et al., Rev. Sci. Inst. **79** 02A316



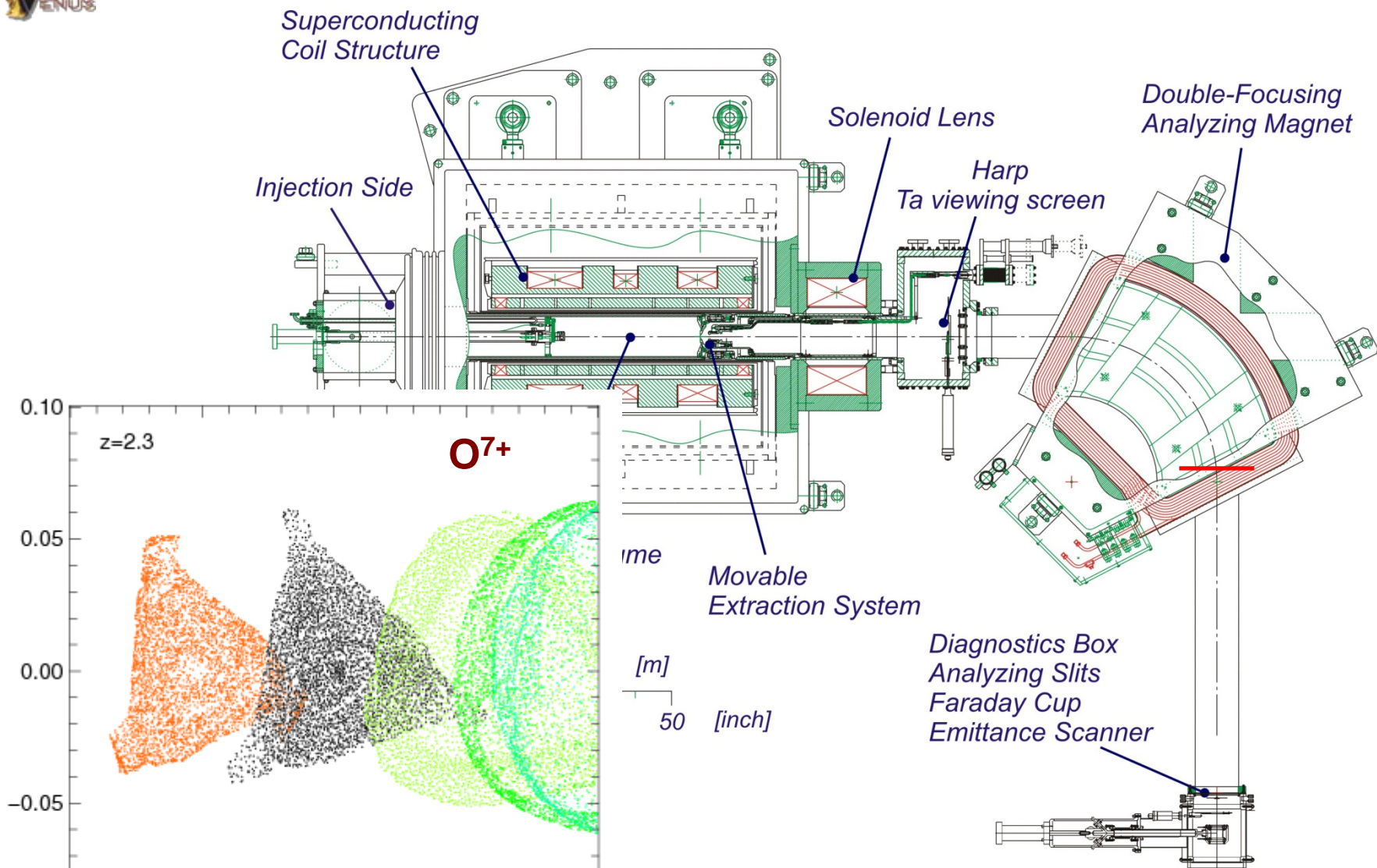
Simulation of oxygen beam extraction and transport



Todd et al., Rev. Sci. Inst. **79** 02A316

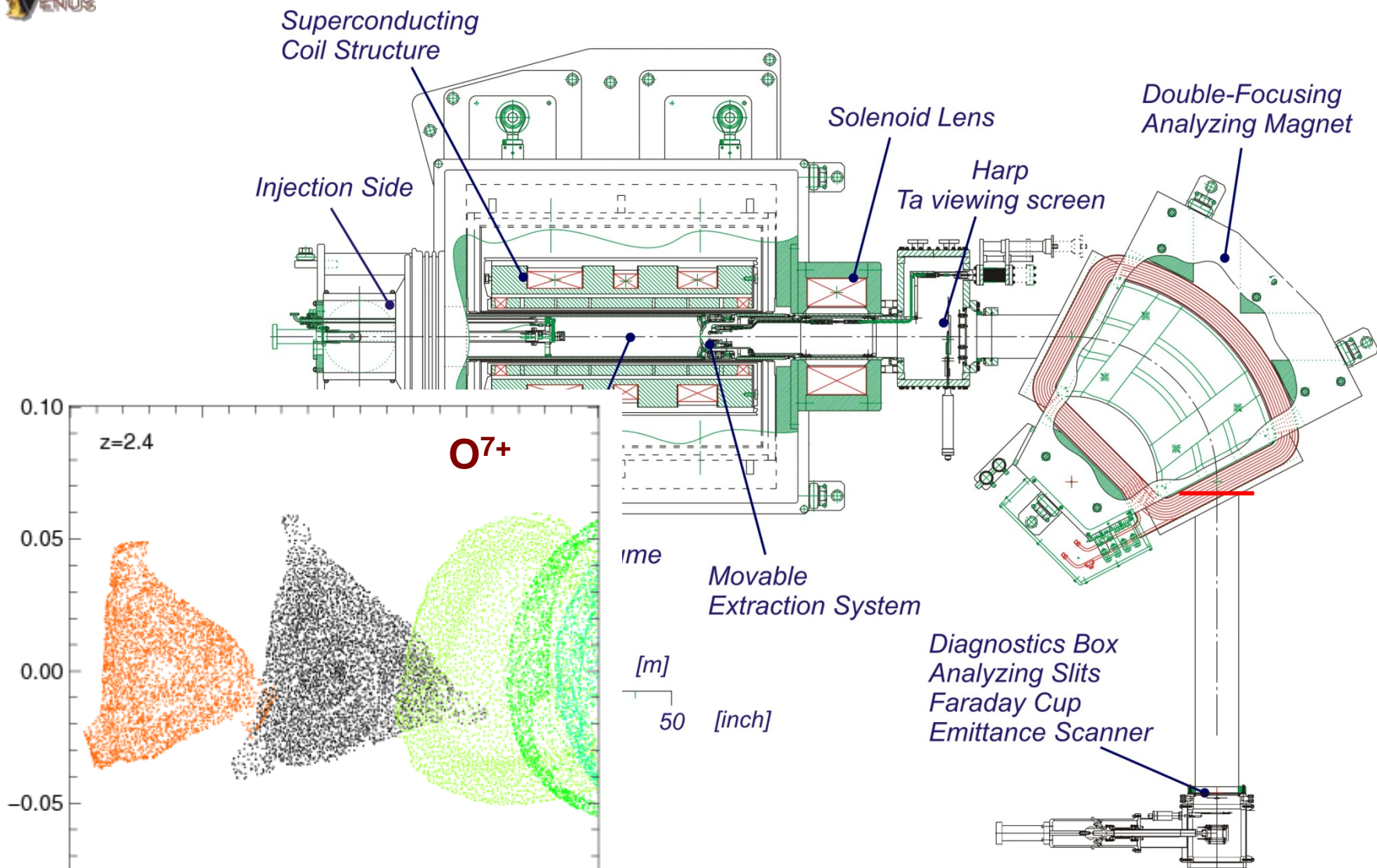


Simulation of oxygen beam extraction and transport



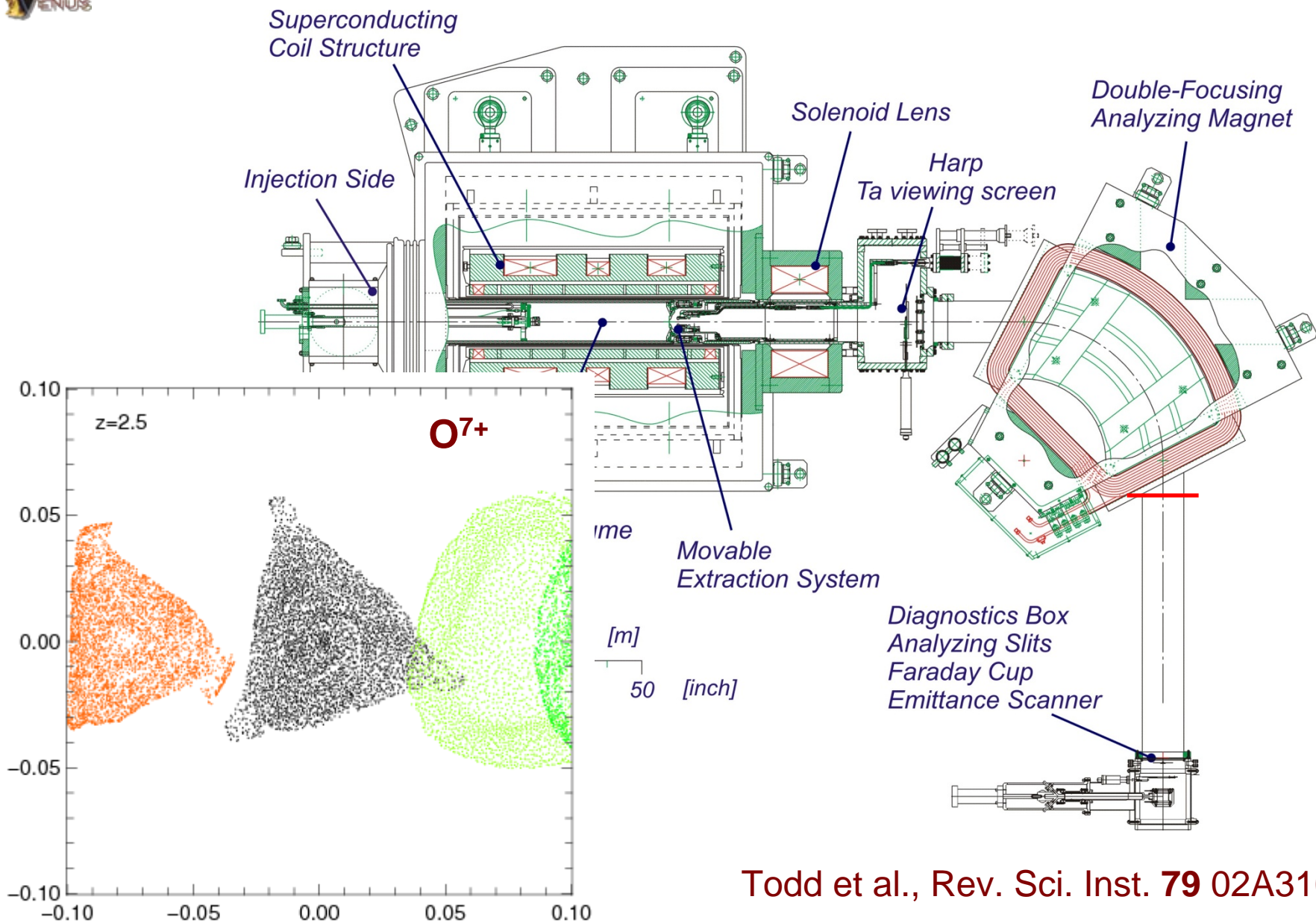


Simulation of oxygen beam extraction and transport



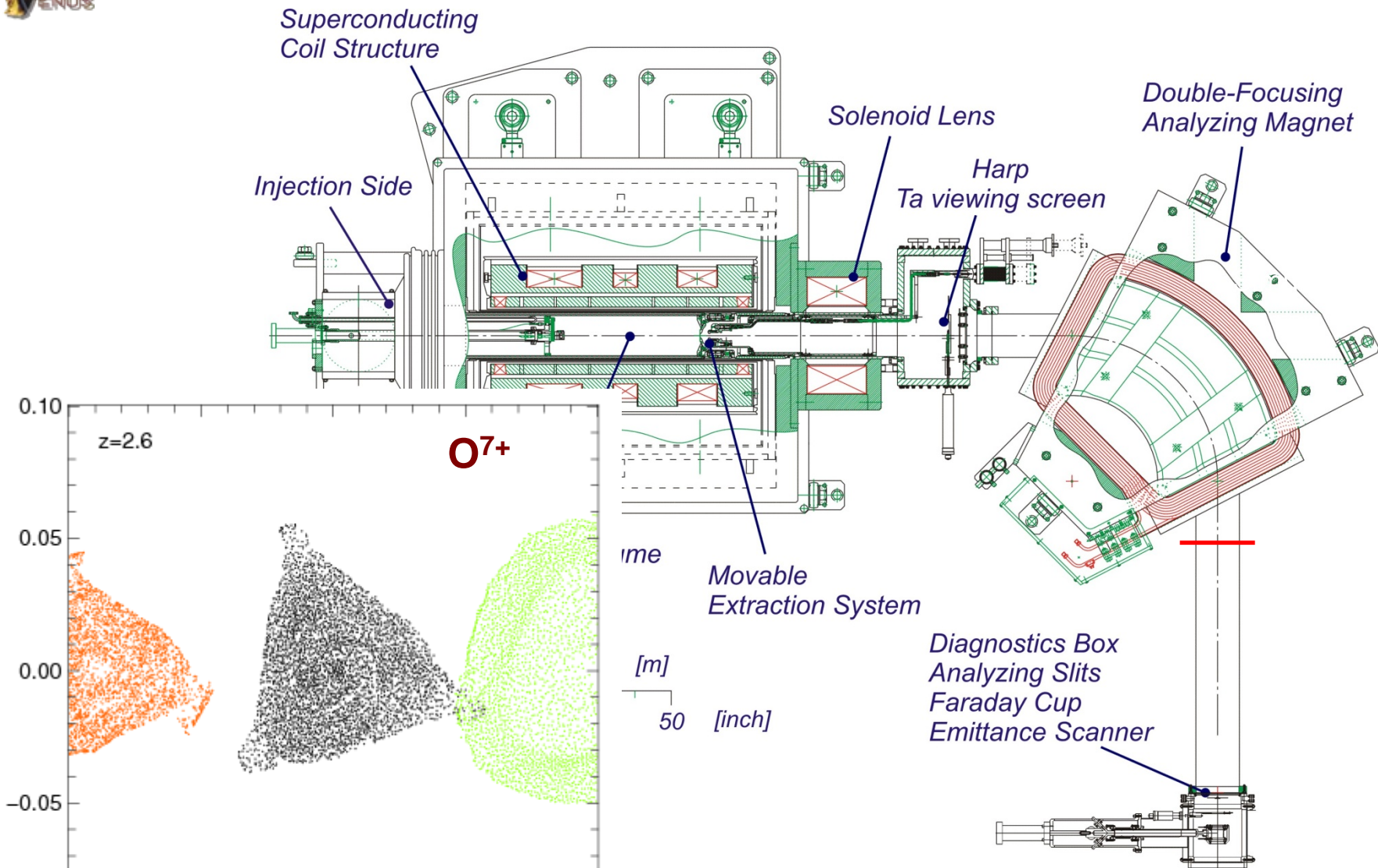


Simulation of oxygen beam extraction and transport





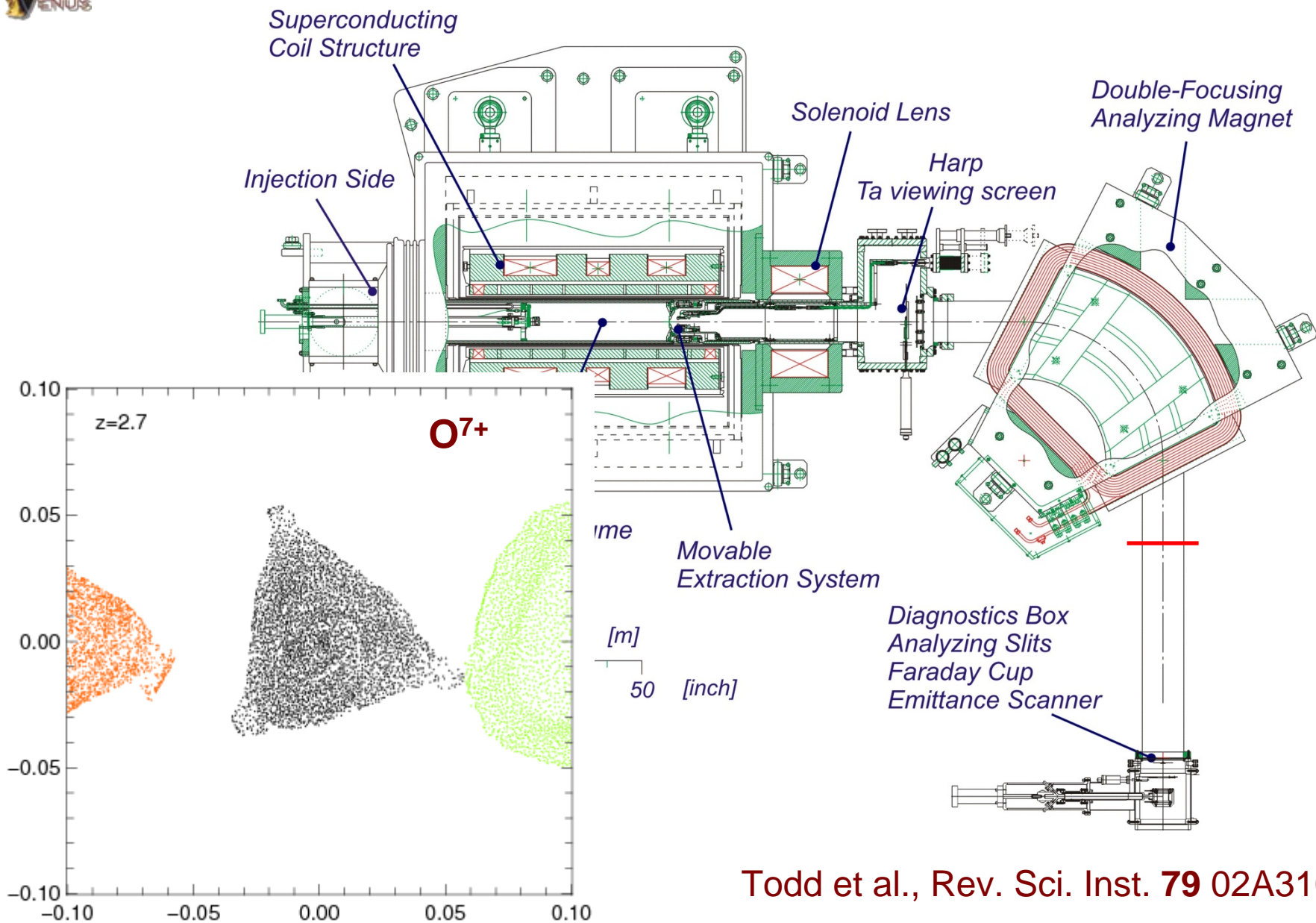
Simulation of oxygen beam extraction and transport



Todd et al., Rev. Sci. Inst. **79** 02A316



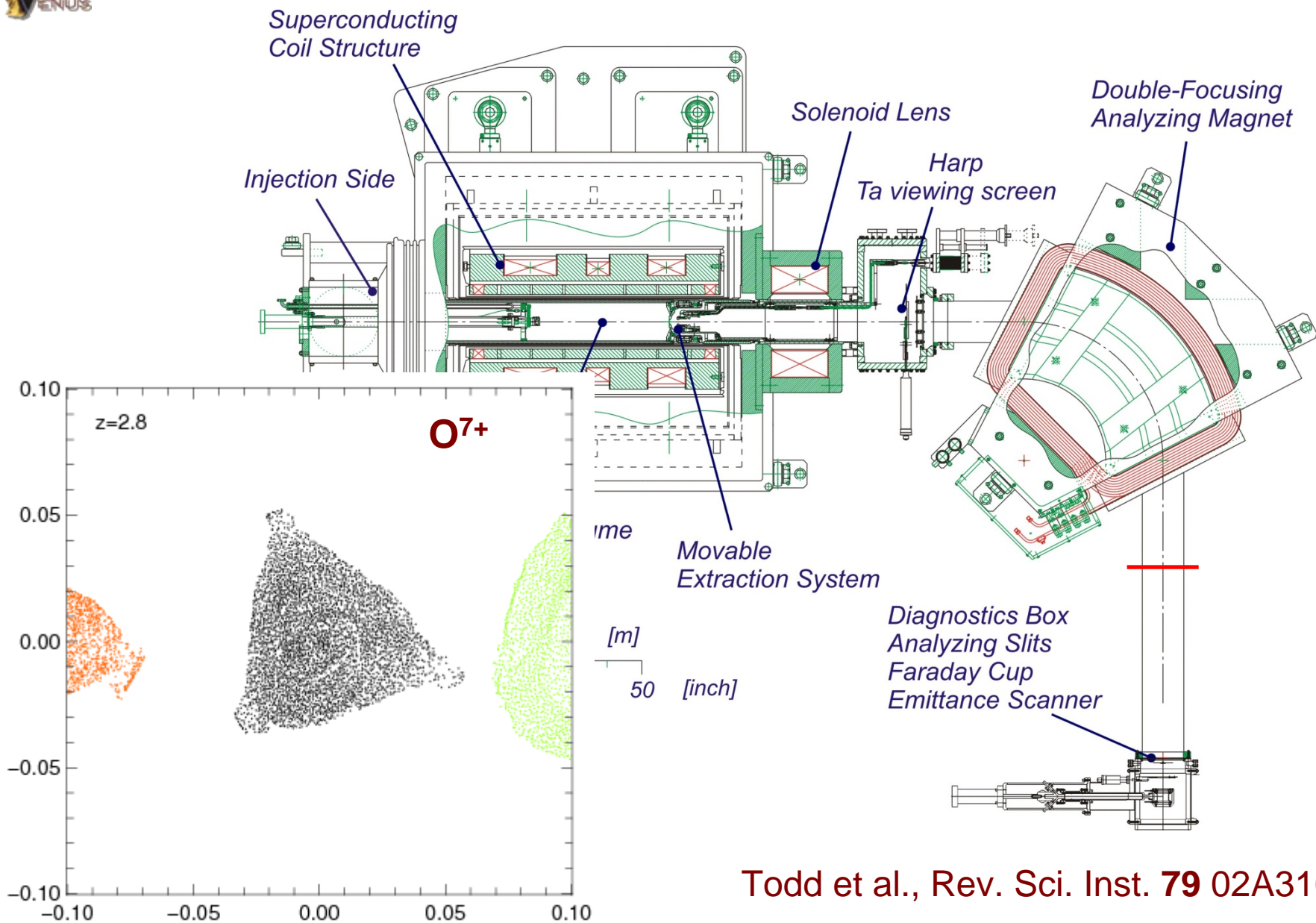
Simulation of oxygen beam extraction and transport



Todd et al., Rev. Sci. Inst. **79** 02A316



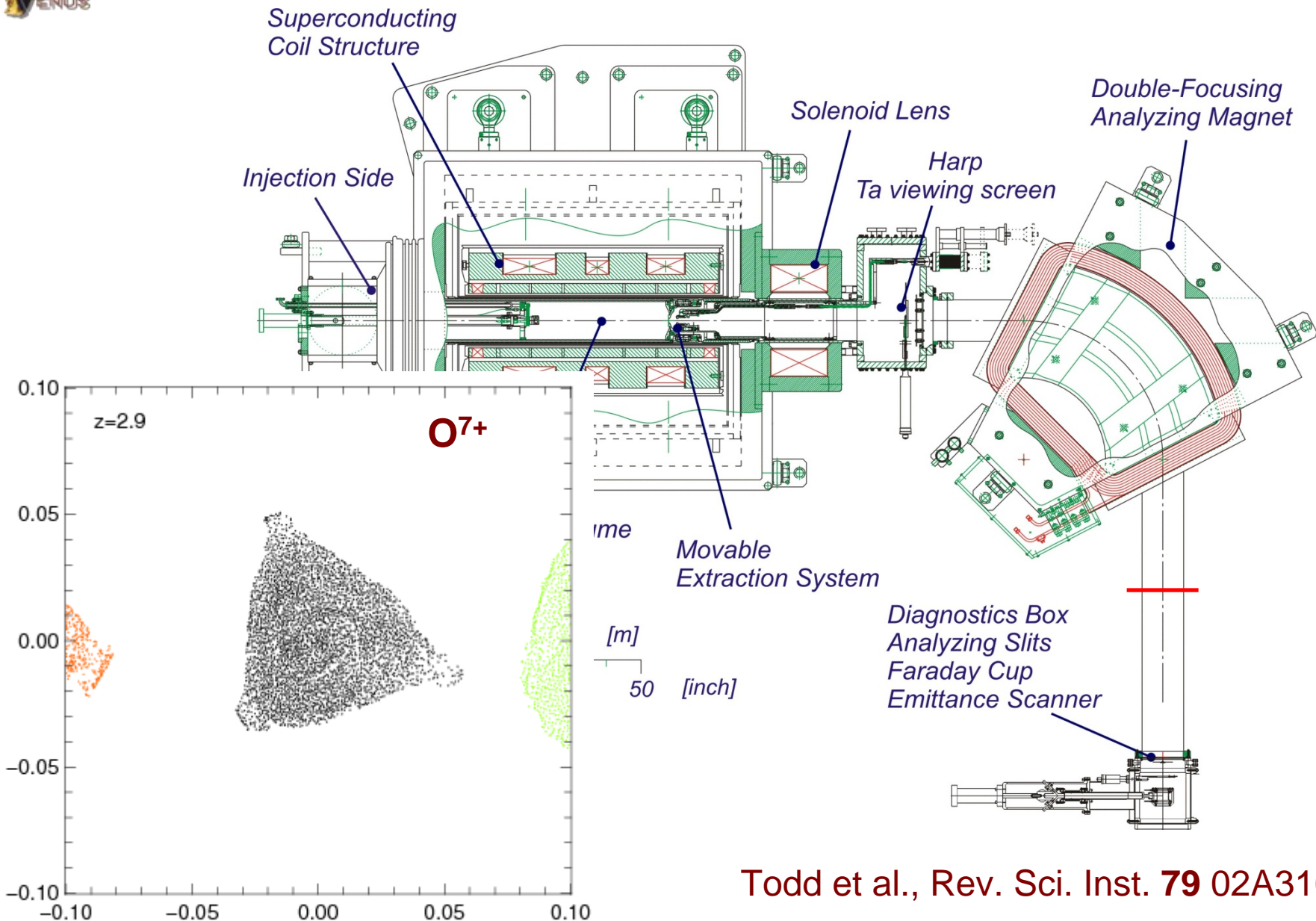
Simulation of oxygen beam extraction and transport



Todd et al., Rev. Sci. Inst. **79** 02A316



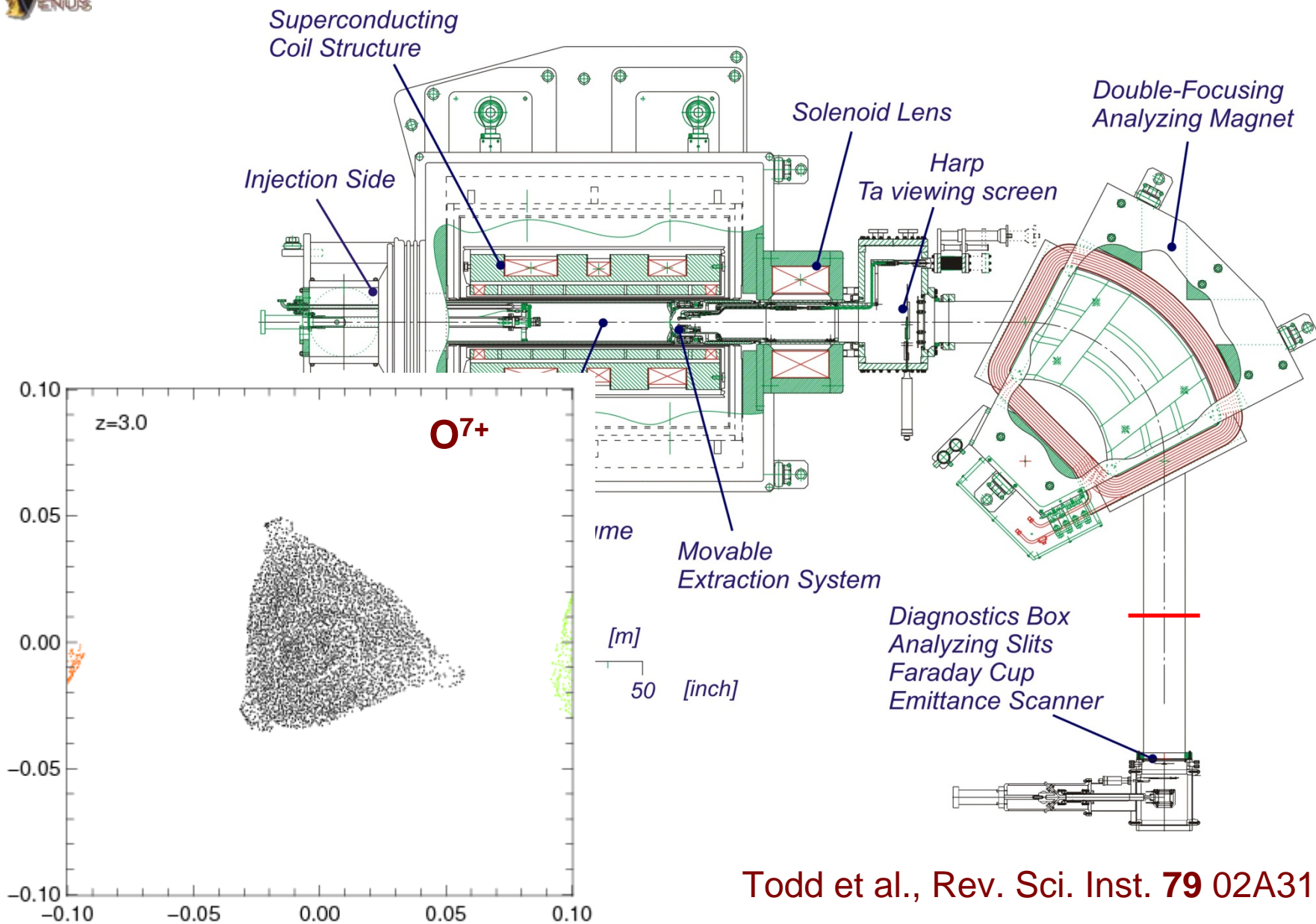
Simulation of oxygen beam extraction and transport



Todd et al., Rev. Sci. Inst. **79** 02A316



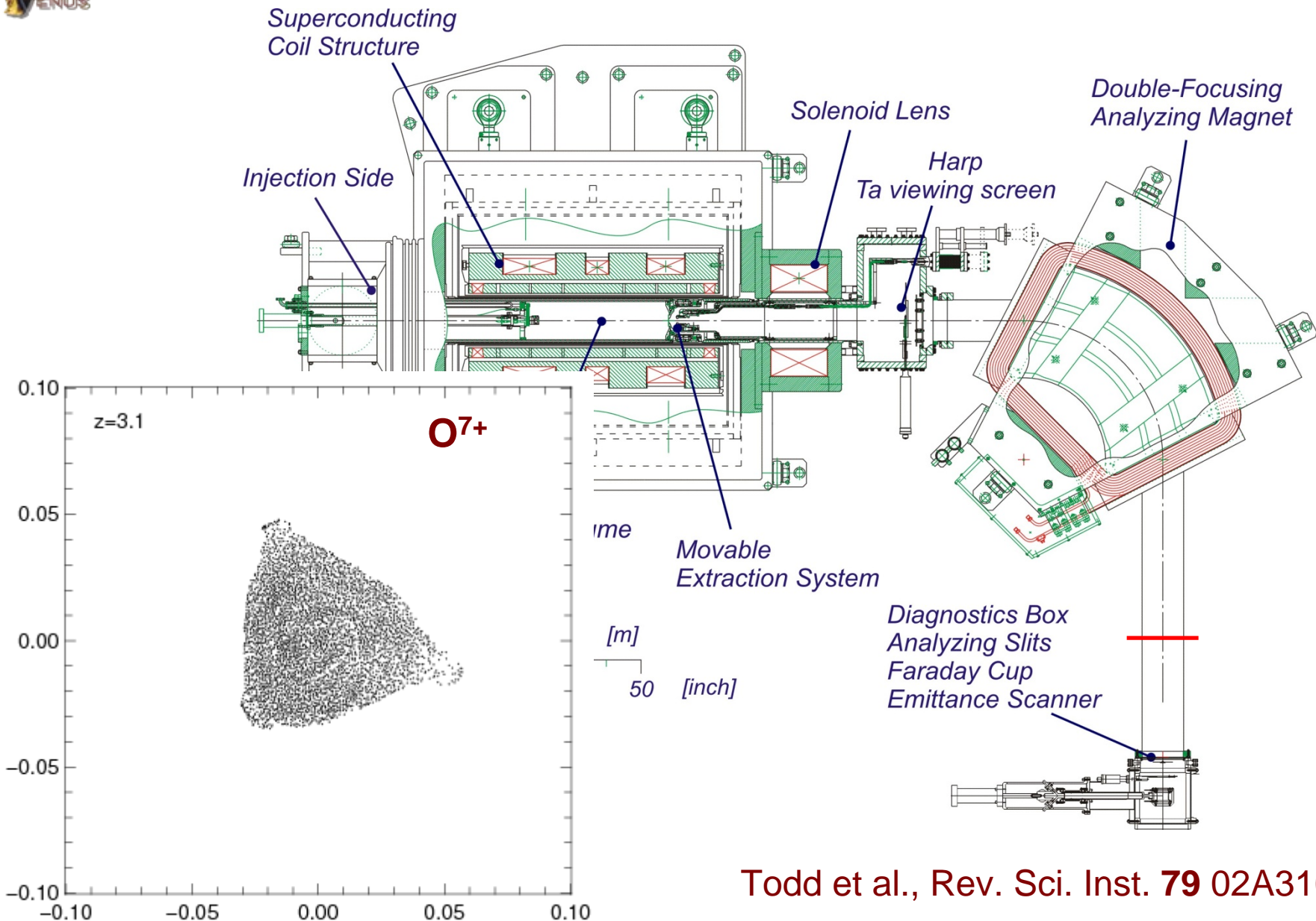
Simulation of oxygen beam extraction and transport



Todd et al., Rev. Sci. Inst. **79** 02A316



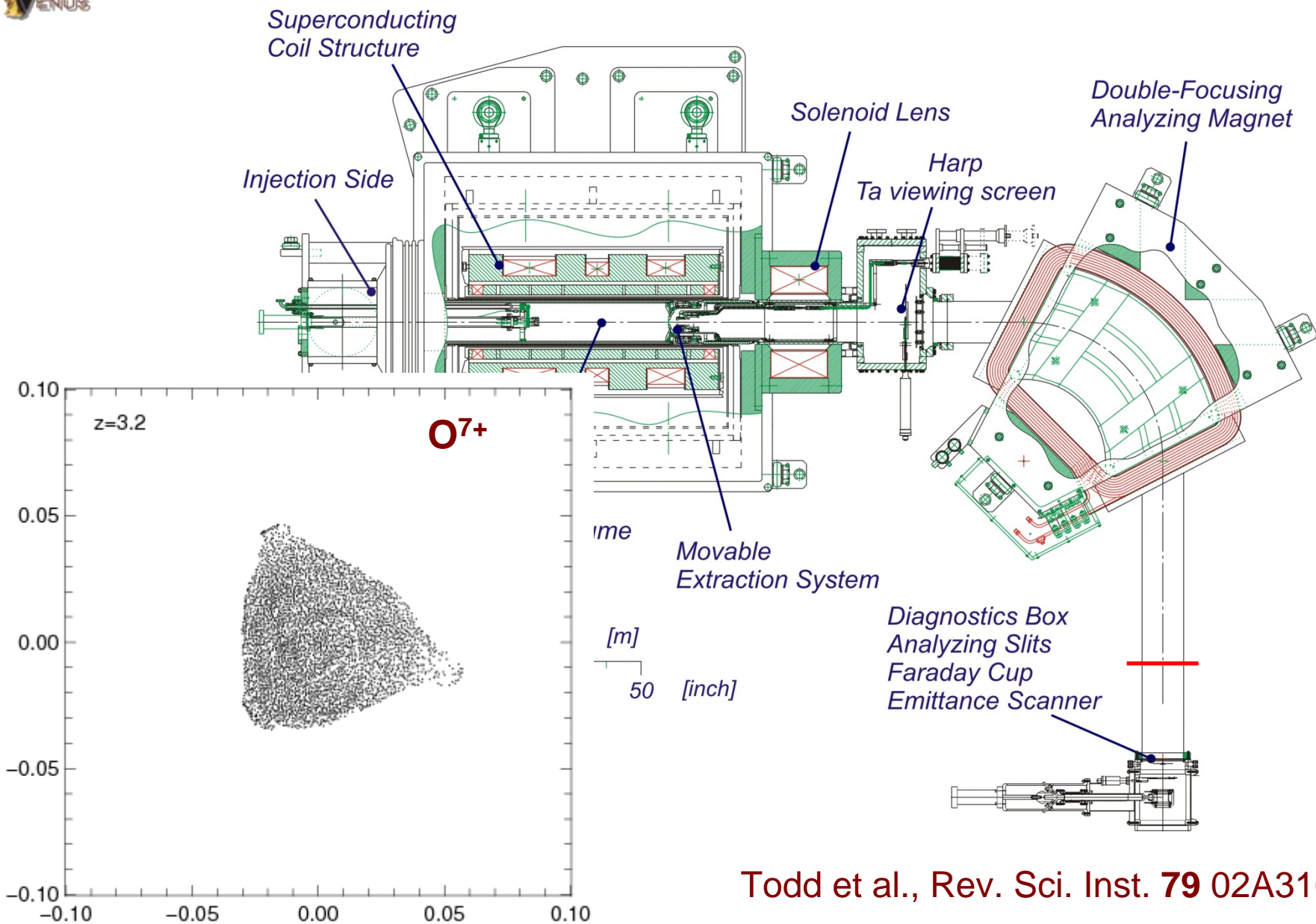
Simulation of oxygen beam extraction and transport



Todd et al., Rev. Sci. Inst. **79** 02A316

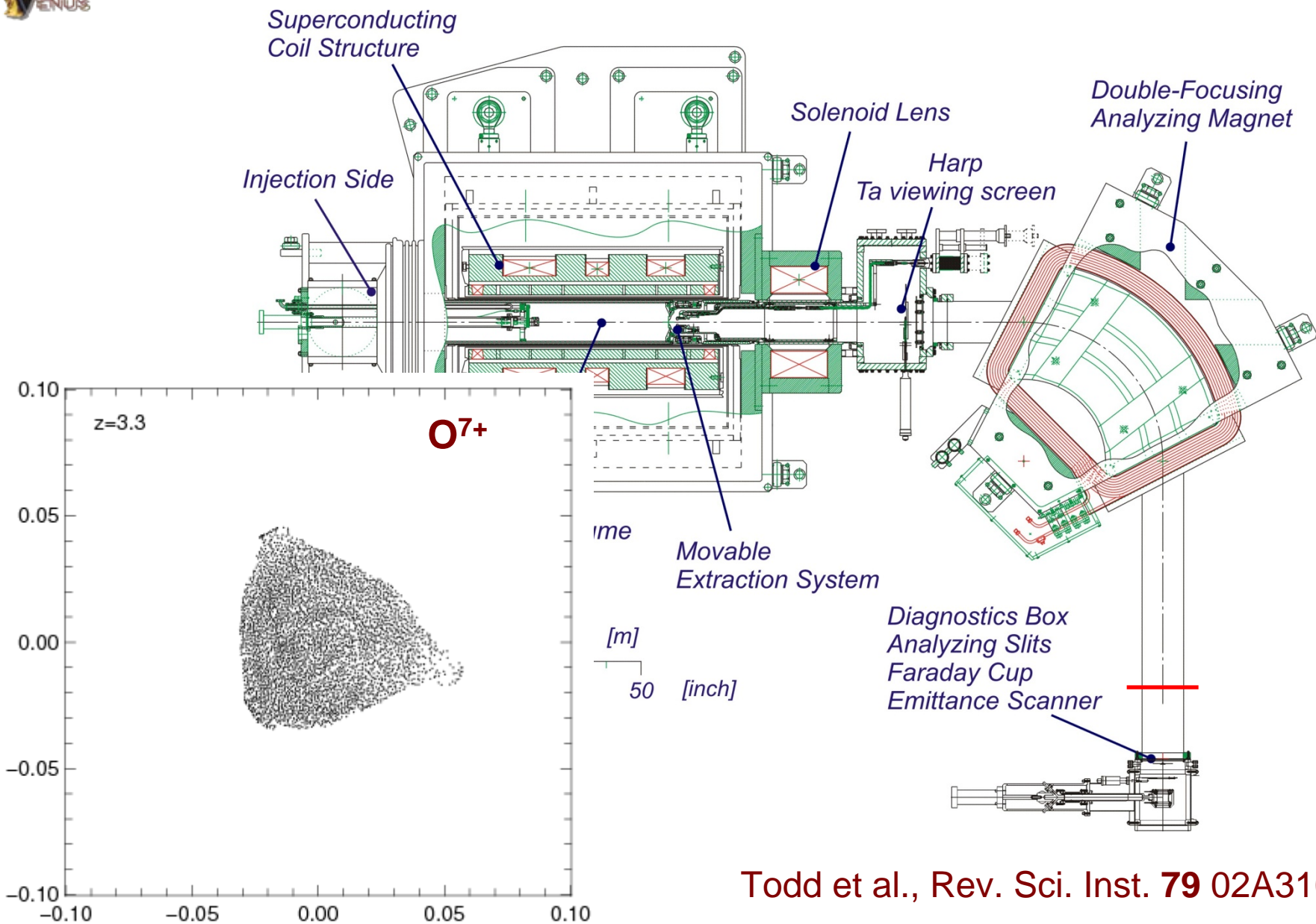


Simulation of oxygen beam extraction and transport





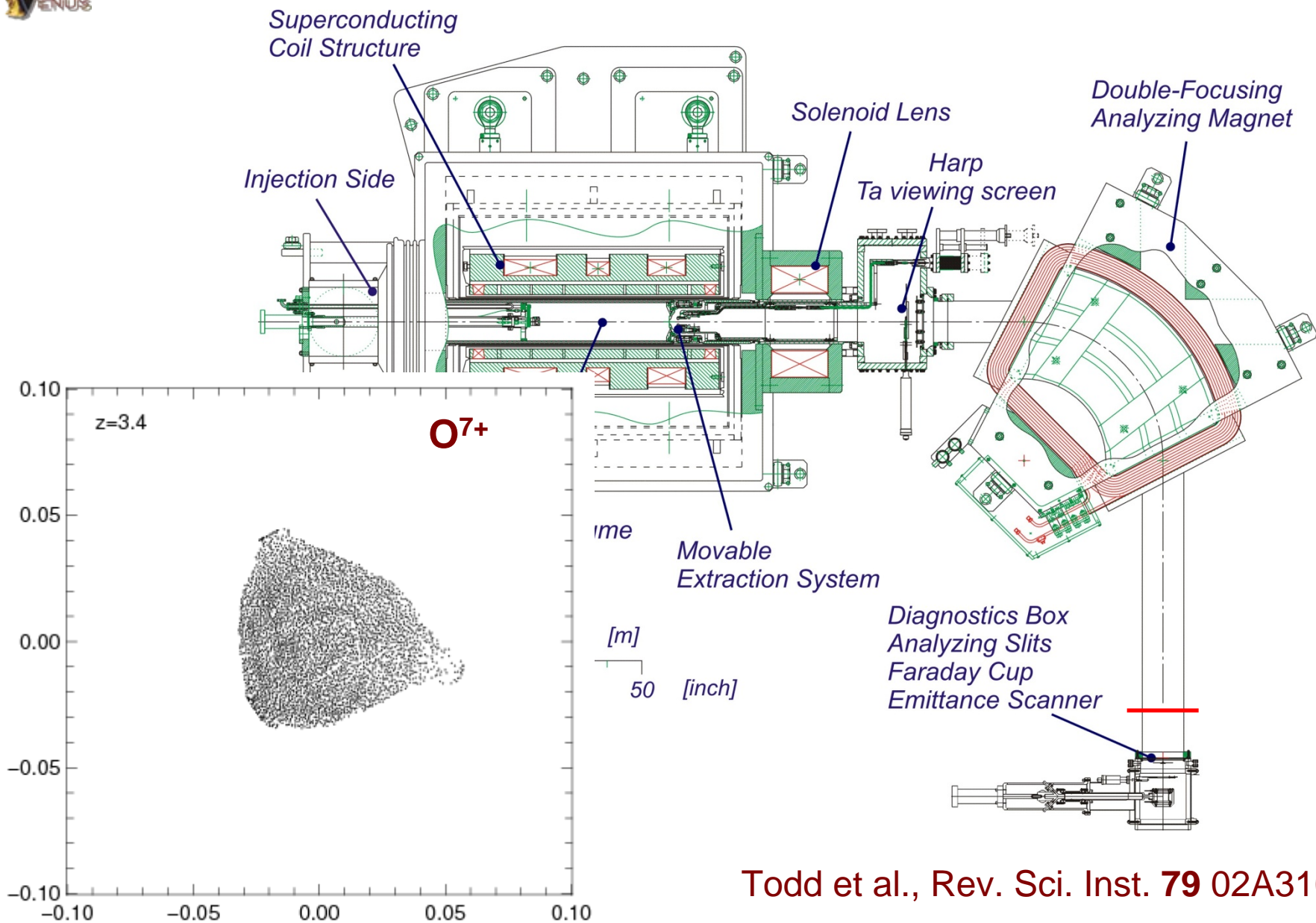
Simulation of oxygen beam extraction and transport



Todd et al., Rev. Sci. Inst. **79** 02A316

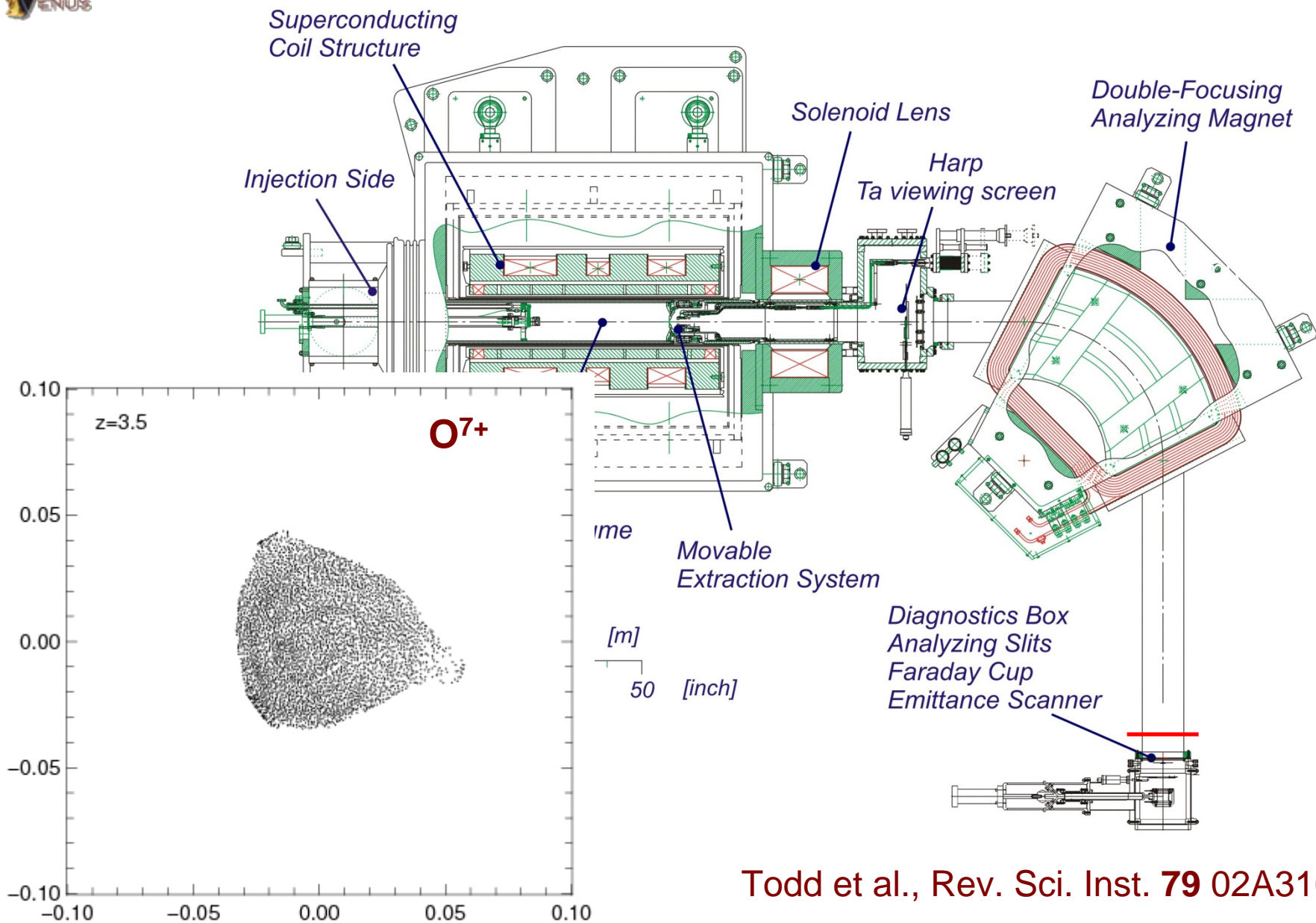


Simulation of oxygen beam extraction and transport



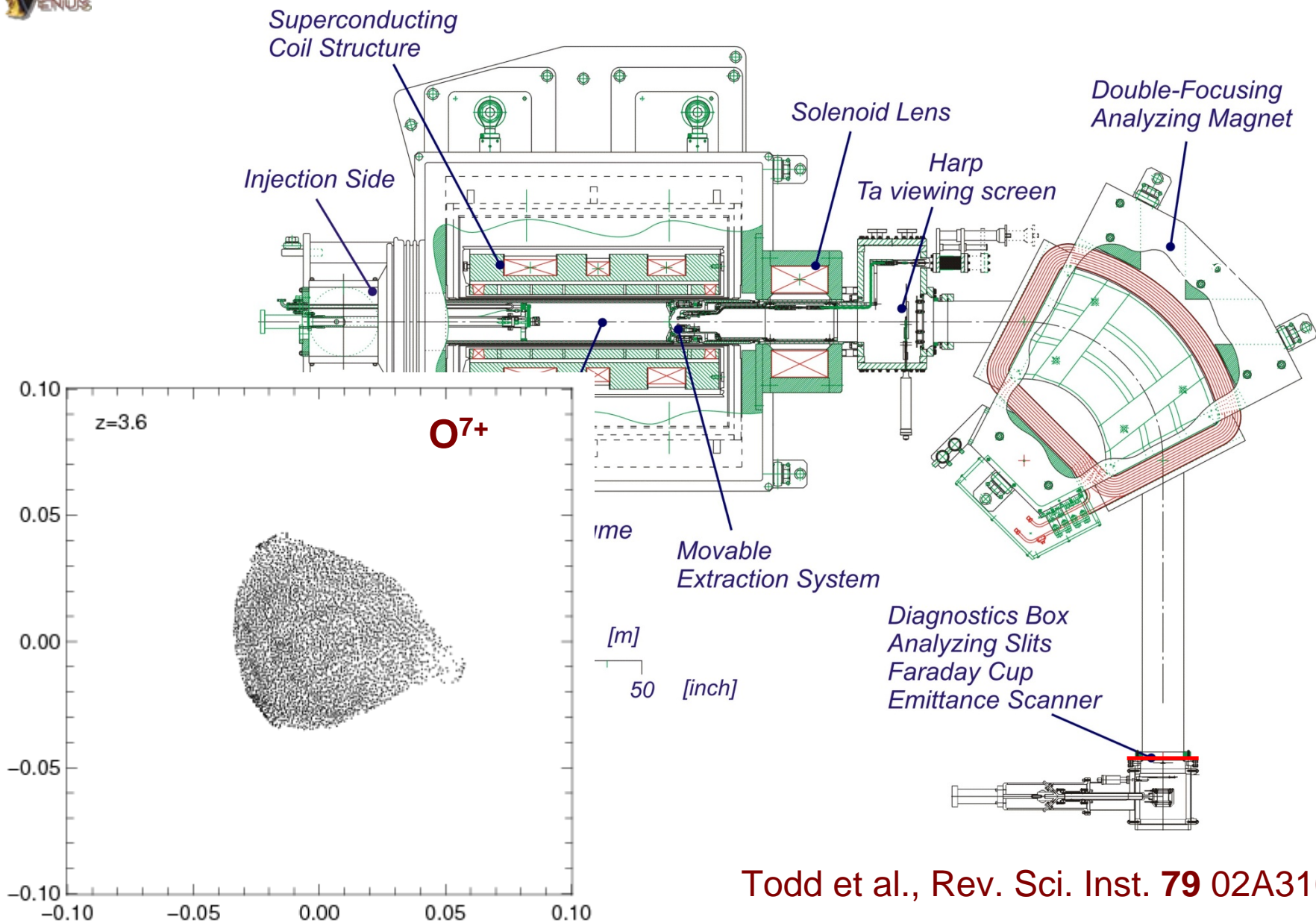


Simulation of oxygen beam extraction and transport



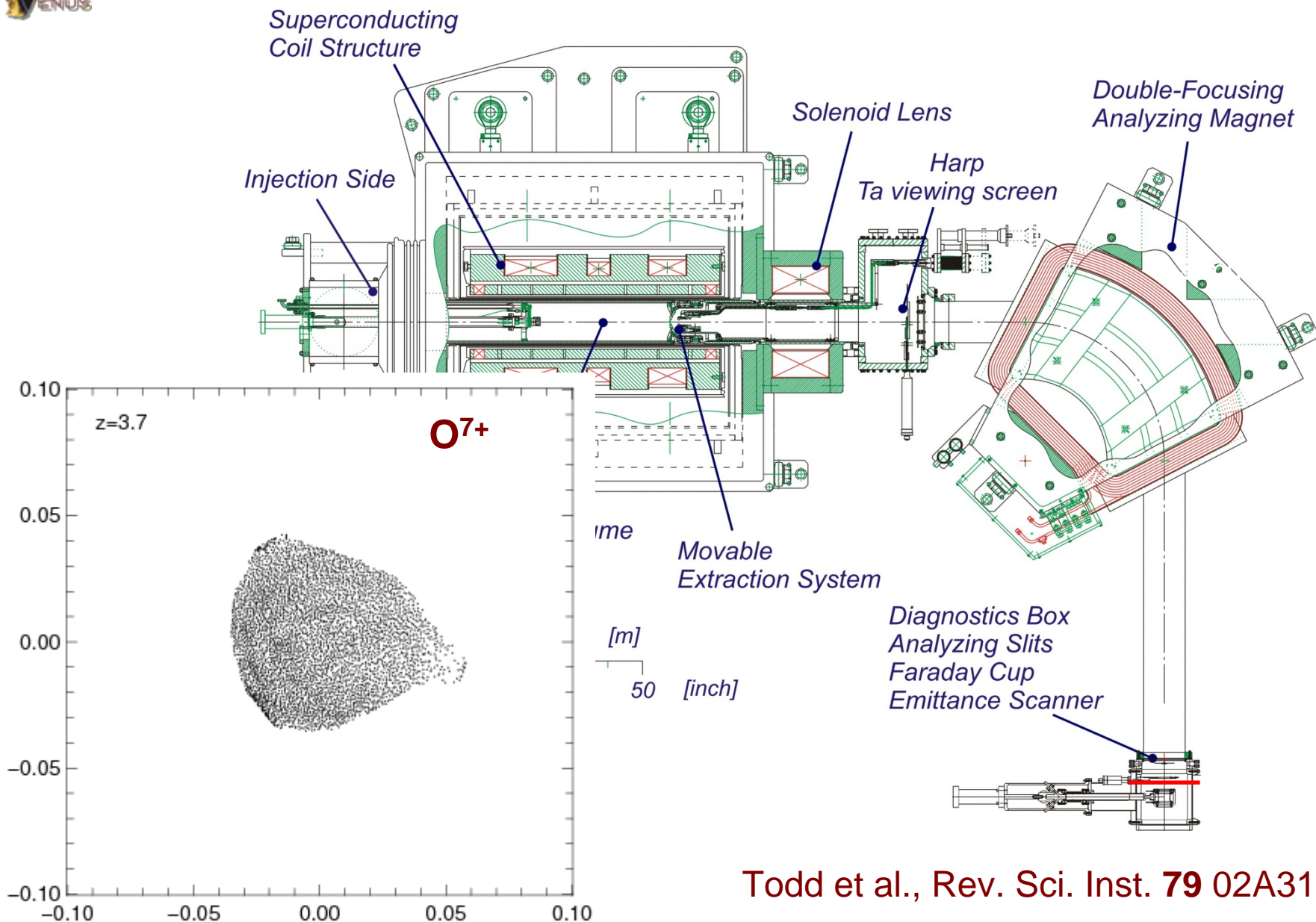


Simulation of oxygen beam extraction and transport





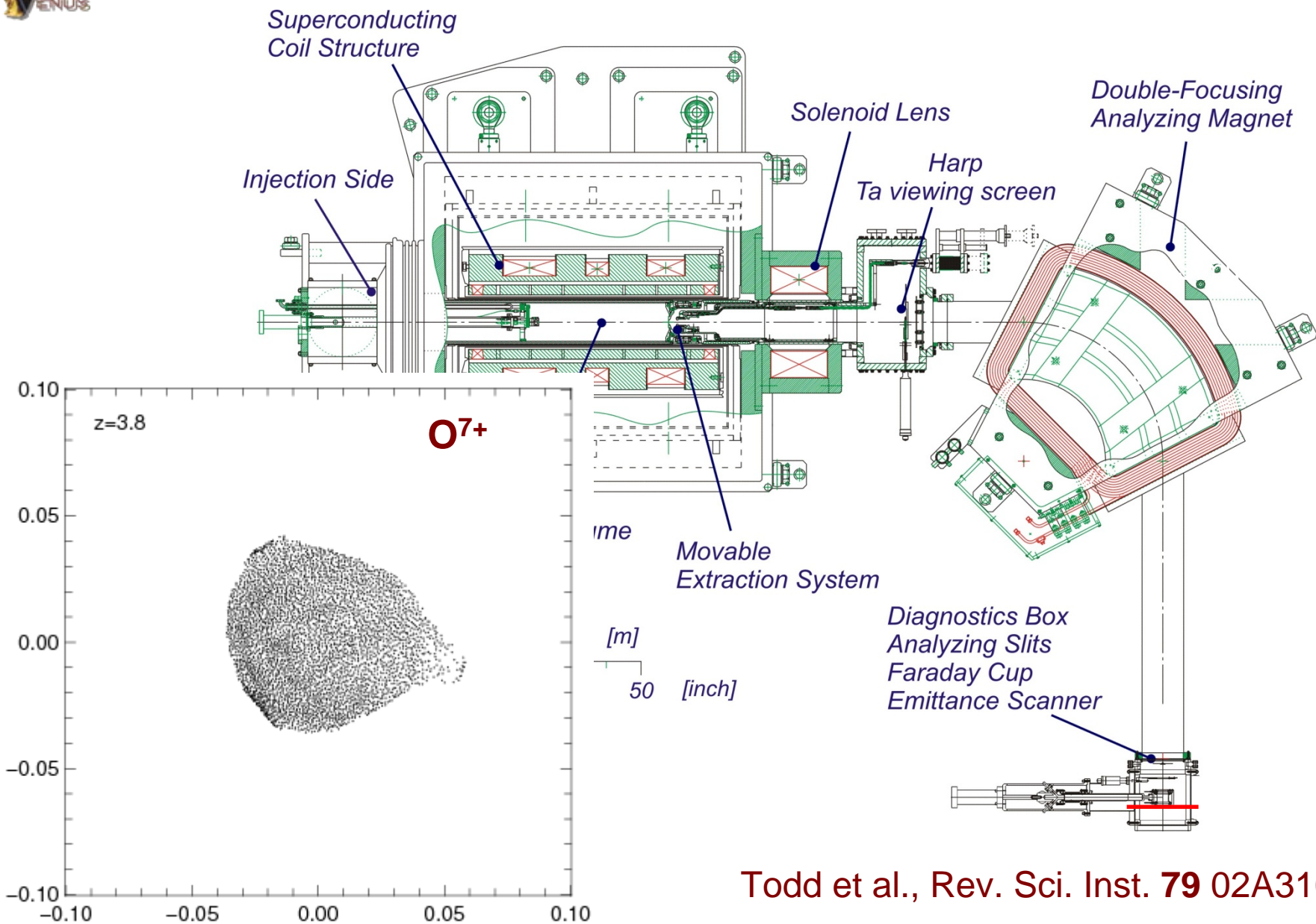
Simulation of oxygen beam extraction and transport



Todd et al., Rev. Sci. Inst. **79** 02A316

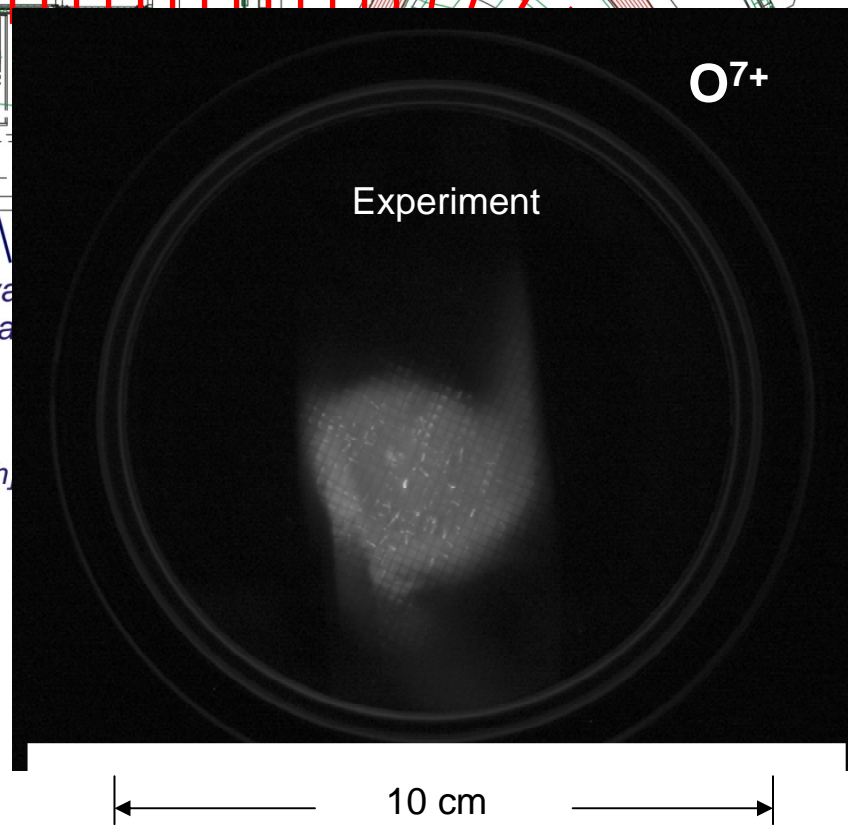
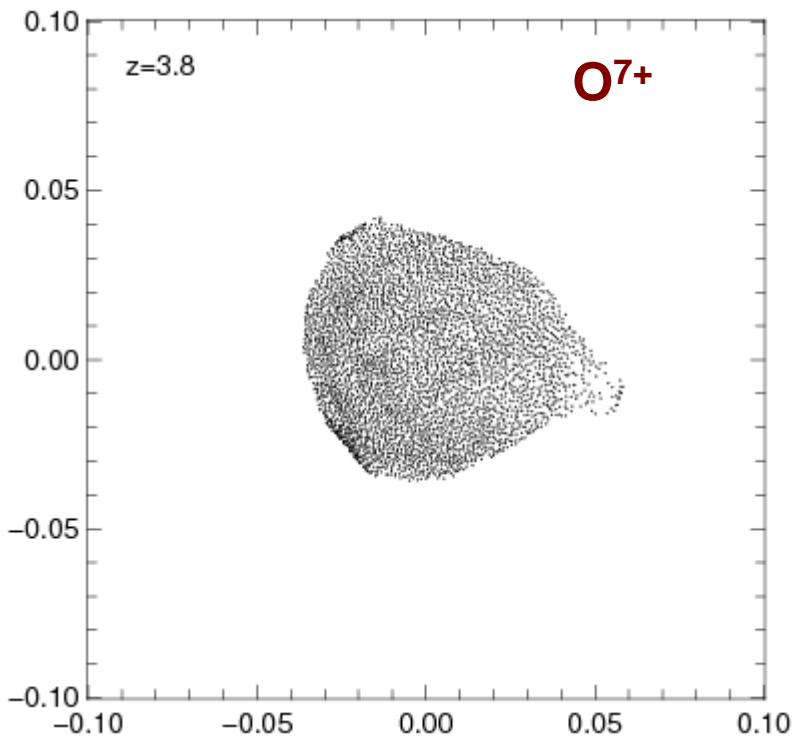
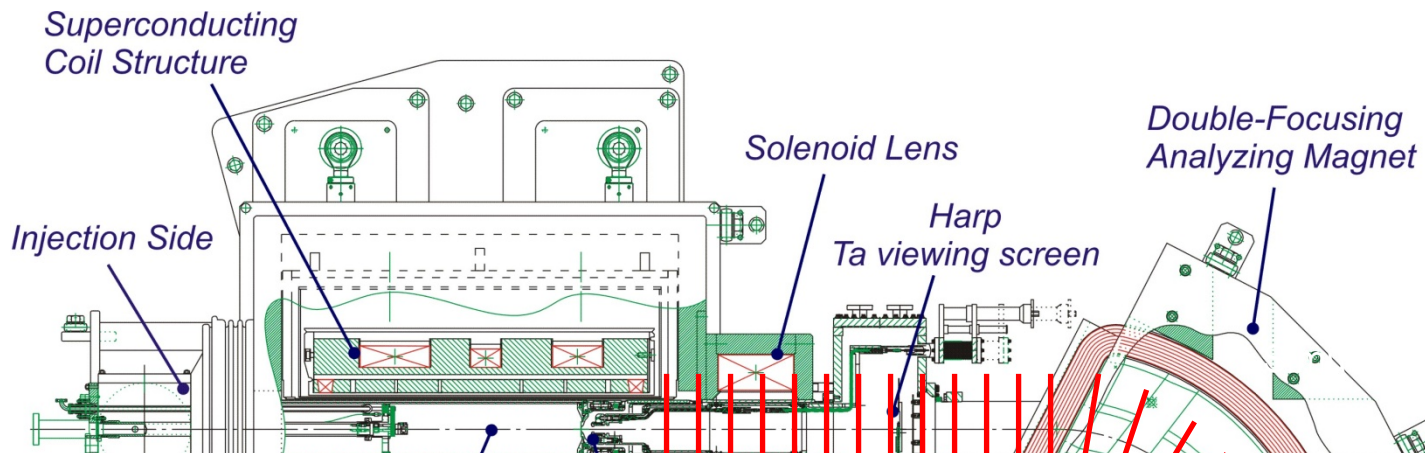


Simulation of oxygen beam extraction and transport





Simulation of oxygen beam extraction and transport





Summary

- The requirements of the next generation heavy ion accelerator continue to drive ECR ion source development
- Higher magnetic fields and higher frequencies are the key to higher performance
- 200e μ A of U³³⁺ and U³⁴⁺ have been produced, high temperature oven development is key for long term production
- 56 GHz ECR ion source magnet structures are feasible with current NbSn₃ technology
- Development should start now to be ready for operation in 5-10 years
- Understanding of the plasma physics and the beam transport is important for the design of the next generation superconducting ECR ion sources

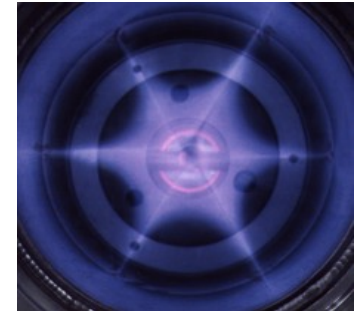
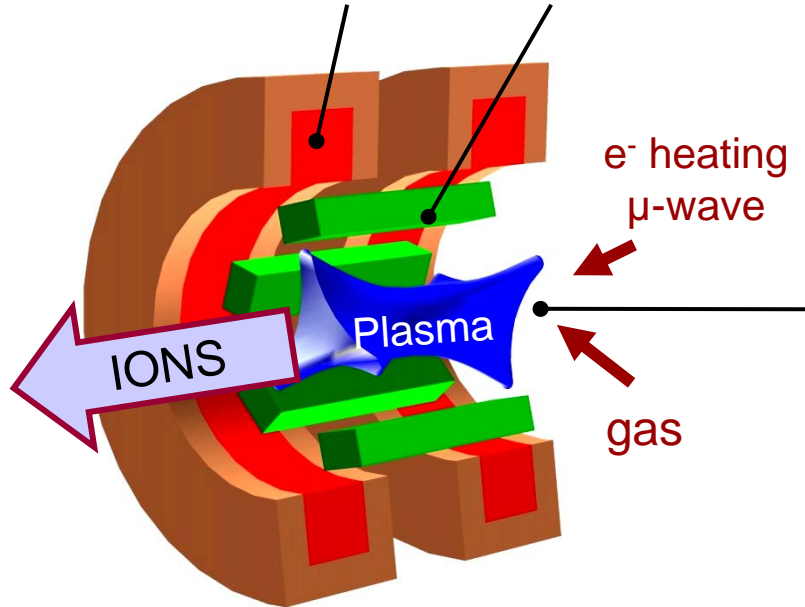
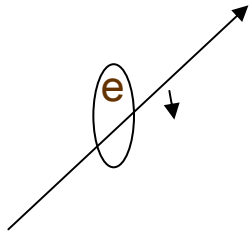
Key parameters for an ECR ion source performance

Plasma is resonantly heated with microwaves

Solenoids and Sextupole form a minimum-B field confinement structure

$$\omega_e = \frac{e \cdot B}{m} = \omega_{rf}$$

Magnetic flux line



$$q \cdot v \cdot B = m \cdot \omega^2 \cdot r$$

$$r = \frac{m \cdot v}{q \cdot B}$$

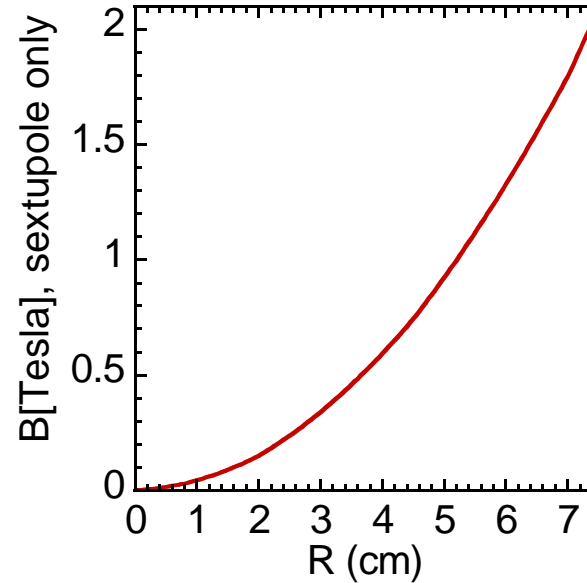
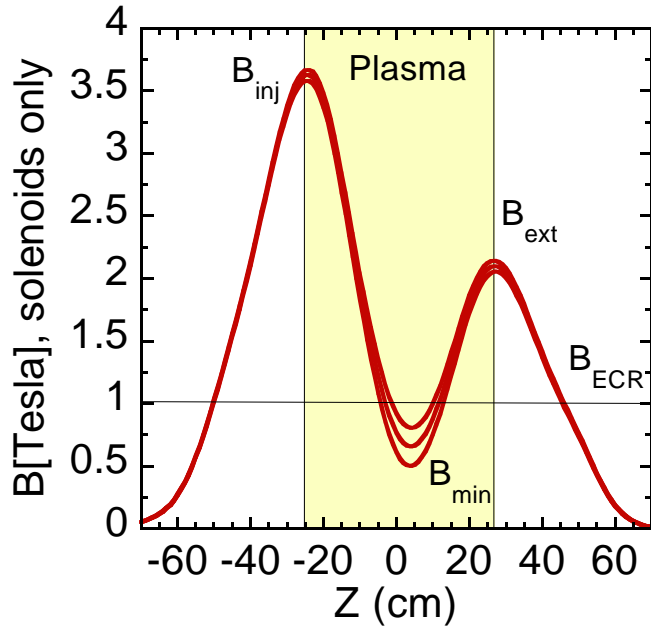
f=28 GHz, B= 1T

r_{Lamor}=0.01...1 mm

Key parameters	
Ion confinement times τ_i	~ms
Plasma densities n_e	$10^9 - 10^{12} /\text{cm}^3$
Electron temperature T_e	eV to MeV
Charge exchange/ neutral gas density σ_{ex}	$q^{1.17} \cdot I_p^{-2.76} \cdot 10^{-12} \text{cm}^2$

Superconducting Magnets: ECR Design 'Standard Model'

28 GHz VENUS Tune

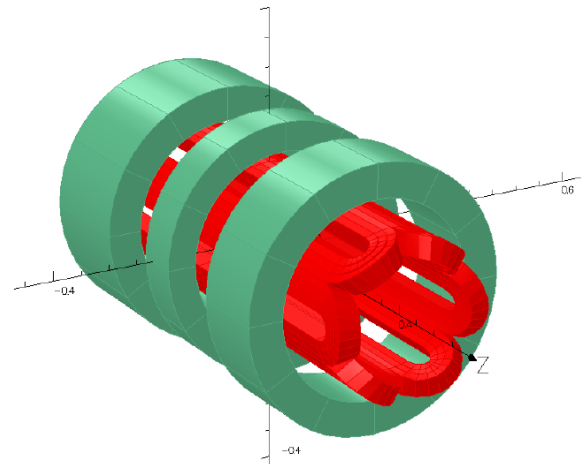


$$B_{inj} \sim 4 \cdot B_{ecr}$$

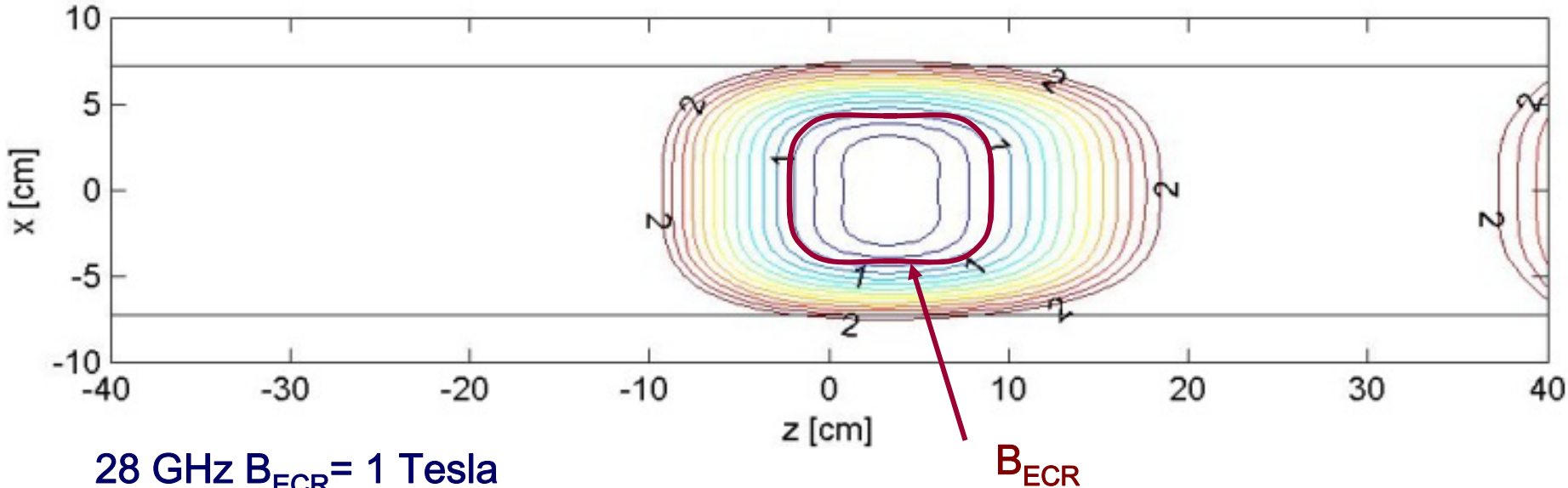
$$B_{min} \sim 0.8 B_{ecr}$$

$$B_{ext} \sim B_{rad}$$

$$B_{rad} \geq 2 B_{ecr}$$



Superconducting Magnets: ECR Design 'Standard Model'



28 GHz $B_{\text{ECR}} = 1$ Tesla

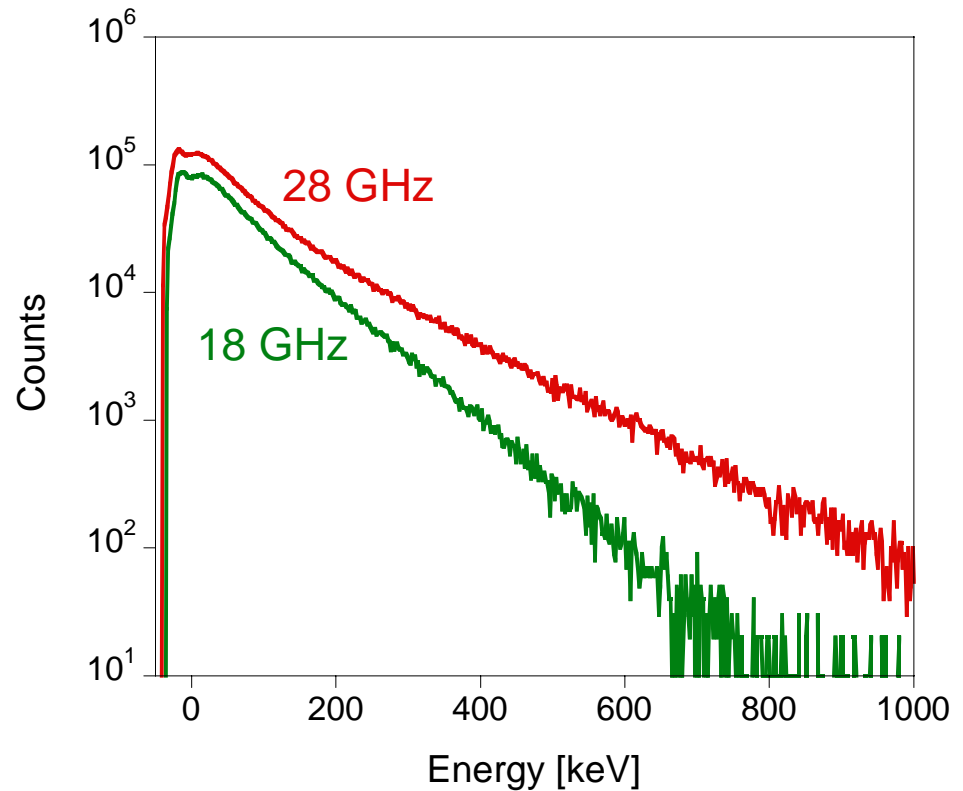
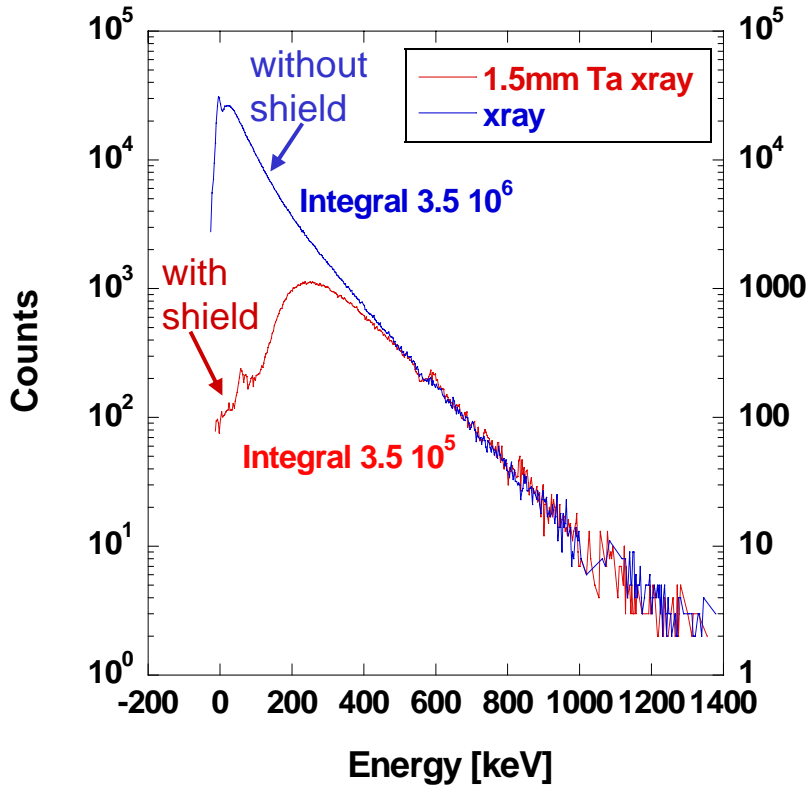
56 GHz $B_{\text{ECR}} = 2$ Tesla

	28 GHz	56 GHz
$B_{\text{inj}} \sim 4 \cdot B_{\text{ecr}}$	4T	8T
$B_{\text{min}} \sim 0.8 B_{\text{ecr}}$.5-.8 T	1-1.6 T
$B_{\text{ext}} \sim B_{\text{rad}}$	2T	4T
$B_{\text{rad}} \geq 2 B_{\text{ecr}}$	2T	4T

Magnetic Design		28 GHz	56 GHz
Max solenoid field	on the coil	6 T	12 T
	on axis	4 T	8 T
Max sextupole field	on the coil	7 T	15 T
	on plasma wall	2.1 T	4.2 T
Superconductor		NbTi	Nb ₃ Sn



The high energy tail of the x-ray spectrum increases substantially at the higher microwave frequency



The scaling of the electron energy temperature with frequency has important consequences for 4th generation superconducting ECR ion source with frequencies of 37GHz, 56GHz.

Several (10s of) watts of cooling power must be reserved for the cryostat.